AD-A191 014 SURVEY OF THE AIR FORCE P78-2 (SCATHA) SATELLITE PLASMA 1/1
WAVE DATA DURING ELECTRON GUN OPERATIONS(U) NAVAL
POSTGRADUATE SCHOOL MONTEREY CA D R LOWERY DEC 87
UNCLASSIFIED F/G 22/1 NL

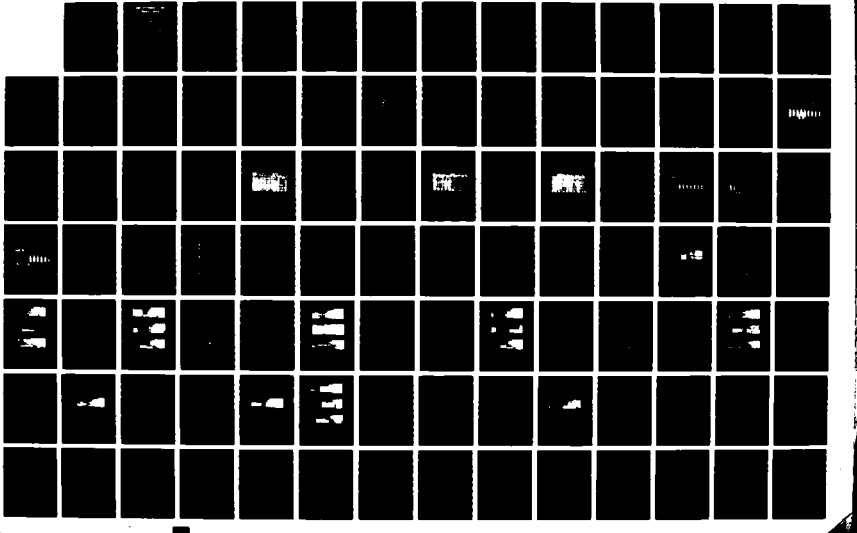

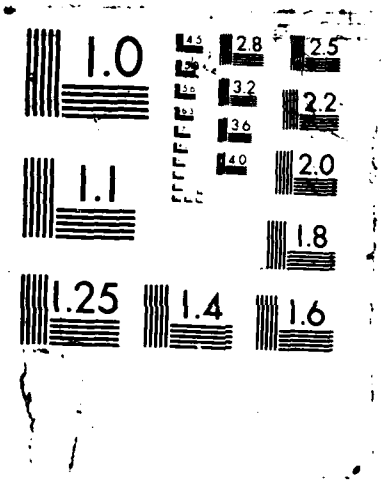
1.0
1.1
1.25
1.4
1.6
1.8
2.0
2.2
2.5
2.8
3.2
3.6
4.0

NAVAL POSTGRADUATE SCHOOL
Monterey, California

THESIS

Survey of the Air Force P78-2 (SCATHA) Satellite Plasma Wave Data During Electron Gun Operations

by

Donald Ray Lowery

December 1987

Thesis Advisor: R.C. Olsen

UNCLASSIFIED
SECURITY CLASSIFICATION OF THIS PAGE

REPORT DOCUMENTATION PAGE

A191 014

1a. REPORT SECURITY CLASSIFICATION UNCLASSIFIED	1b. RESTRICTIVE MARKINGS
2a. SECURITY CLASSIFICATION AUTHORITY	3. DISTRIBUTION / AVAILABILITY OF REPORT Approved for public release; distribution is unlimited.
2b. DECLASSIFICATION / DOWNGRADING SCHEDULE	
4. PERFORMING ORGANIZATION REPORT NUMBER(S)	5. MONITORING ORGANIZATION REPORT NUMBER(S)
6a. NAME OF PERFORMING ORGANIZATION Naval Postgraduate School 6b. OFFICE SYMBOL (If applicable) 61	7a. NAME OF MONITORING ORGANIZATION Naval Postgraduate School
6c. ADDRESS (City, State, and ZIP Code) Monterey, Ca. 93943	7b. ADDRESS (City, State, and ZIP Code) Monterey, Ca. 93943
8a. NAME OF FUNDING / SPONSORING ORGANIZATION 8b. OFFICE SYMBOL (If applicable)	9. PROCUREMENT INSTRUMENT IDENTIFICATION NUMBER
8c. ADDRESS (City, State, and ZIP Code)	10. SOURCE OF FUNDING NUMBERS PROGRAM ELEMENT NO. / PROJECT NO. / TASK NO / WORK UNIT ACCESSION NO.

11. TITLE (Include Security Classification)
SURVEY OF THE AIR FORCE P78-2 (SCATHA) SATELLITE PLASMA WAVE DATA DURING ELECTRON GUN OPERATIONS

12. PERSONAL AUTHOR(S)
Lowery, Donald R.

13a. TYPE OF REPORT	13b. TIME COVERED	14. DATE OF REPORT (Year, Month, Day)	15. PAGE COUNT
Master's thesis	FROM 87 Jun TO 87 Dec	1987 December	96

16. SUPPLEMENTARY NOTATION

17. COSATI CODES			18. SUBJECT TERMS (Continue on reverse if necessary and identify by block number)
FIELD	GROUP	SUB-GROUP	Satellite, SCATHA, Electron Cyclotron Frequency, gyrofrequency, Stimulated Plasma Waves, Electron Beam, Electron Gun

19. ABSTRACT (Continue on reverse if necessary and identify by block number)

The Air Force P78-2 satellite, known as SCATHA, was designed to study spacecraft charging processes at geosynchronous orbit. This thesis examines the plasma wave data taken during two periods when active experiments were conducted with the electron gun. Emissions at the electron gyrofrequency were stimulated by the operation of the electron gun on some occasions. These indicate interaction between the electron beam and plasma at local resonant frequencies of the plasma.

A major objective of this thesis is to catalogue the characteristics of the plasma wave data common to the modes of operation of the electron gun. The purpose is to provide a baseline for analysis of data not only from SCATHA, but from other spacecraft including the space shuttle orbiter. Stimulated emissions at characteristic frequencies dependent on gun current and voltage were identified. These were consistently observed during the

20. DISTRIBUTION / AVAILABILITY OF ABSTRACT ☒ UNCLASSIFIED/UNLIMITED ☐ SAME AS RPT. ☐ DTIC USERS	21. ABSTRACT SECURITY CLASSIFICATION UNCLASSIFIED
22a. NAME OF RESPONSIBLE INDIVIDUAL Dr. R.C. Olsen	22b. TELEPHONE (Include Area Code) 408-646-2019 22c. OFFICE SYMBOL 610S

DD FORM 1473, 84 MAR 83 APR edition may be used until exhausted.
All other editions are obsolete

SECURITY CLASSIFICATION OF THIS PAGE
UNCLASSIFIED

☆ U.S. Government Printing Office: 1986—606-24.

19 (cont)
experiment presented here, and other events analyzed but not displayed.

Approved for public release; distribution is unlimited.

Survey of the Air Force P78-2 (SCATHA) Satellite Plasma Wave Data During Electron Gun Operations

by

Donald Ray Lowery
Lieutenant Commander, United States Navy
B.S.E.E. North Carolina State University, 1975

Submitted in partial fulfillment of the requirements for the degree of

MASTER OF SCIENCE IN ENGINEERING SCIENCE

from the

NAVAL POSTGRADUATE SCHOOL
December 1987

Author: Donald Ray Lowery
Donald Ray Lowery

Approved by: Chris Olsen
Dr. R. C. Olsen, Thesis Advisor

Dr. S. Gnanalingam, Second Reader

K E Woehler
Dr. K. Woehler, Chairman
Department of Physics

G E Schacher
Dr. Gordon E. Schacher
Dean of Engineering and Science

ABSTRACT

The Air Force P78-2 satellite, known as SCATHA, was designed to study spacecraft charging processes at geosynchronous orbit. This thesis examines the plasma wave data taken during two periods when active experiments were conducted with the electron gun. Emissions at the electron gyrofrequency were stimulated by the operation of the electron gun on some occasions. These indicate interaction between the electron beam and plasma at local resonant frequencies of the plasma.

A major objective of this thesis is to catalogue the characteristics of the plasma wave data common to the modes of operation of the electron gun. The purpose is to provide a baseline for analysis of data not only from SCATHA, but from other spacecraft including the space shuttle orbiter. Stimulated emissions at characteristic frequencies dependent on gun current and voltage were identified. These were consistently observed during the experiment presented here, and other events analyzed but not displayed.

TABLE OF CONTENTS

LIST OF FIGURES

LIST OF TABLES

I. INTRODUCTION

A. PROBLEM OF SATELLITE CHARGING

1. Satellite Charging

Satellite charging is the buildup of static electrical charge on the surface of satellites and has become an important issue in the use of satellite systems. Large negative potentials occur due to an imbalance between ambient electron and ion currents and currents generated by photoemission and secondary electrons. Spacecraft charging effects have been observed on several satellites over the past few years (DeForest, 1972), (Garrett, 1981), (Grard, 1983) and (Olsen, 1985). The large negative potentials that have been induced on geosynchronous satellites have been linked to the satellite failures and unexpected mode changes that have been observed periodically over the past several years. These anomalies can be directly attributed to spacecraft charging effects, which create arcing on the satellite surface, resulting in material breakdown and subsequent failure of the satellite. Figure I-1 shows the correlation between observed satellite

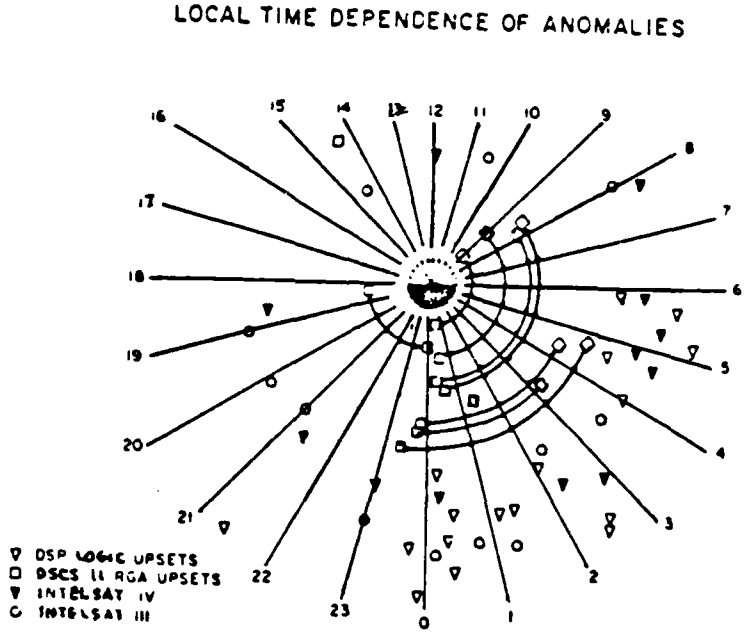

Figure I-1. Local time plot of satellite operations anomalies.

anomalies and the satellite local time (Grard, et al, 1983). It can be seen that a majority of the satellite anomalies occurred during the midnight to dawn period. Also of immediate concern is the effect of satellite charging on plasma measurements (Garrett, 1981).

B. EXPERIMENTS

1. As a result of satellite charging effects, active potential control on ATS 5 and ATS 6 has been attempted by use of ion and electron sources (Olsen, 1981) and (Olsen, 1985) and on SCATHA using an electron beam source (Olsen, 1987). The SCATHA program was specifically designed to study the effects of spacecraft charging and to determine the effects on the satellite and the near satellite environment through a series of carefully designed experiments. In particular, this thesis deals with the plasma wave observations during SCATHA electron gun experiments. Reports on such observations are rare in the published literature.

Stimulated plasma waves in the VLF range are reported by Akai (ISAS RN285) and Kawashima, et al, (1976) for the Japanese satellite, Jikiken (EXOS-B). Electron gun experiments were conducted to study the wave excitation phenomena (both linear and non-linear) due to beam-plasma

interactions, and to control satellite potential by electron beam emission. The electron gun current was stepped from .25 - 1.0 mA in .25 mA increments. The gun voltage was stepped from 100 to 200 volts in 25 volt increments. The plasma waves were classified by type based on the L-region in which they were observed. Waves at the electron gyrofrequency and its harmonics, the upper hybrid resonance frequency and the plasma frequency were observed.

Kawashima, et al, (1982) reported results of electron beam experiments from ionospheric sounding rockets K-10-11 and K-10-12. VLF and HF waves were excited by the beam and plasma heating was observed in Langmuir probe and electrostatic analyzer measurements. Kawashima, et al, (1987) reported VLF waves excited by electron beam operations on the Japan-US tether rocket experiment CHARGE-2.

Koons and Cohen (1982) reported plasma waves and electrical discharges stimulated by an electron beam on SCATHA. Correlation between a change in gun parameters and a change to the spectrum was noted. Electrostatic emissions above the electron gyrofrequency were detected on the electric antenna.

Experiments on ISEE-1 used beam currents of 10-60 μA and beam energies of 0-40 eV. This is comparable to SCATHA data we will present. Lebreton, et al, (1982) reported the enhancement of the electric wave spectrum by the injection of an electron beam on ISEE-1. No clearly identified resonances were reported.

Matasumoto, et al, (1975) reported on new wave phenomena in the VLF range observed by the Japanese sounding rocket K-9M-41. A low energy electron beam was used to investigate the non-linear wave and particle interactions in the ionospheric plasma. Triggered emissions at frequencies around the lower hybrid resonance frequency were found.

Plasma heating as a result of electron beam injections is discussed in Margot-Chaker, et al, (1986). The experiment was conducted on a Black Brant V rocket, AAF-NVB-06 fired through an auroral arc. It was shown that electron beam plasma interactions in the 200-250 km ionosphere resulted in strong electron heating. Beam currents were 1, 10 and 100 mA and beam voltages were 1.9, 4 and 8 kV.

Plasma waves at the plasma frequency and at the electron gyrofrequency generated in the laboratory are discussed by Bernstein, et al, (1975). Electron beam-

plasma interaction is only briefly discussed. This laboratory data was of interest, but tended to deal with the beam-plasma discharge which involves a neutral gas background, not our case.

There have been few reports in the literature of naturally occurring emissions at or near the electron gyrofrequency (Koons and Edgar, 1985). The dispersion relation for electron gyrofrequency harmonic waves does not have a solution at exactly the gyrofrequency. Koons and Edgar, (1985) report detection of emissions by the VLF receiver on SCATHA at and just above the local electron gyrofrequency. They concluded that present theories could not account for the waves that were the subject of their report.

This thesis will examine the plasma wave data taken during two periods when active experiments with the SC4-1 electron gun were being conducted. The effect the operation of the electron gun has on the plasma wave data is described in an attempt to provide a baseline for comparison of future data not only for SCATHA, but for other spacecraft including the space shuttle. Attempts are made to distinguish those characteristics of the plasma wave data that are generated or affected by the

electron gun operations from those that are naturally occurring. Identification of plasma waves stimulated by the electron beam at or near the electron gyrofrequency were a major focus of this investigation.

II. THE SCATHA PROGRAM

A. SATELLITE DESCRIPTION

1. SCATHA Satellite

The Air Force P78-2 satellite (Figure II-1), known as SCATHA for Spacecraft Charging at High Altitudes was launched in January 1979 to study causes and dynamics of spacecraft charging processes at geosynchronous orbit. The satellite was launched into a nearly geosynchronous orbit with a period of 23.5 hours at an apogee of 7.3 Re and a perigee of 5.8 Re. The satellite is cylindrical in shape measuring approximately 1.75 meters long and 1.75 meters wide. It is spin stabilized at about 1 rpm with the spin axis in the plane of the orbit and perpendicular to a line between the earth and sun. The instruments are mostly contained in the bellyband and solar cells cover most of the remaining part of the cylinder (Figure II-2). Also carried on the instrument package were particle detectors and electron and ion guns to be used for charge control experiments. The electron gun experiment is described below. Also included in the scientific package were various instruments to measure the potentials existing near the spacecraft and to detect

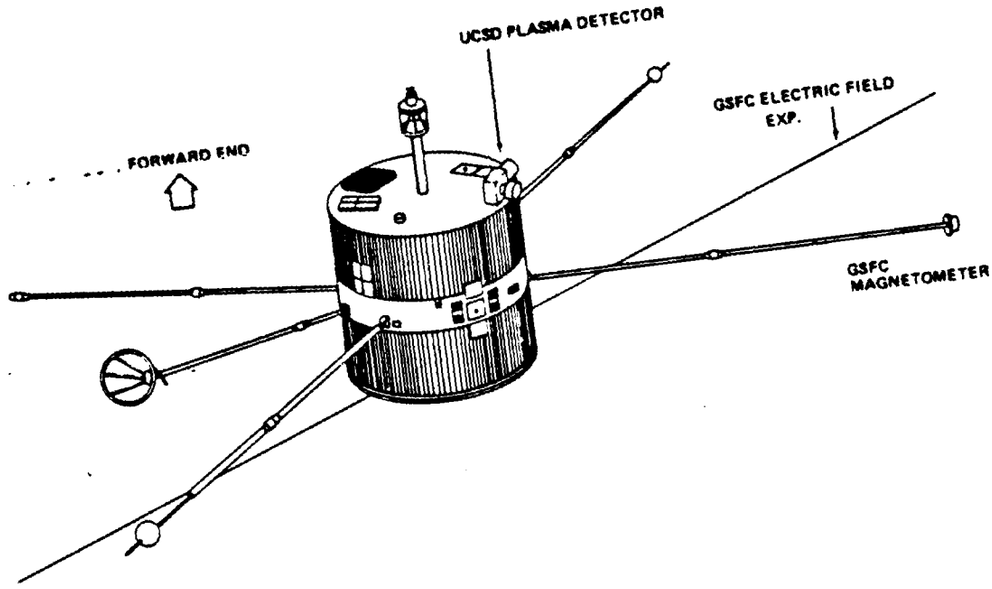

Figure II-1. SCATHA Space Vehicle (P78-2).

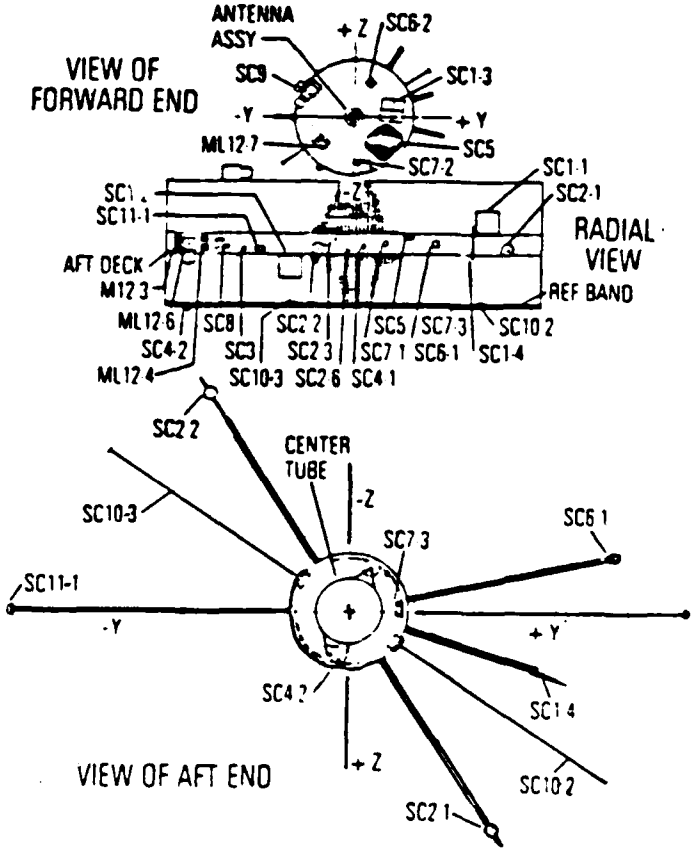

Figure II-2. Experiment and boom locations on the SCATHA satellite.

wave and particle emissions. The scientific instruments are summarized in Table I and the description of the experiments and the principal investigators are found in Fennell. (1982)

Survey of the plasma wave data generated during active electron beam experiments are included in this thesis. Survey of the plasma wave data generated by ion gun experiments is the subject of the Master's thesis of Lt. Leonard Weddle, USN.

The study of spacecraft charging was conducted on the SCATHA satellite to determine the effect of both natural charging of the satellite and attempt to control the spacecraft potential through active experiments. Two periods of plasma wave data generated during electron beam operations are examined in Chapter III.

B. ELECTRON GUN

1. SC4-1 Experiment

The electron beam system (SC4-1) on SCATHA was designed to emit a stream of electrons over a range of beam currents and energies. The electron beam emitter is basically a power triode tube consisting of an indirectly heated cathode, control grid, focusing assembly and an

exit anode at satellite ground. The beam characteristics are summarized as follows:

Beam current levels (mA): .001, .01, .1, 1.0, 6.0, 13.0

Beam energy levels (v): 50, 150, 300, 500, 1500, 3000

Beam duty cycles: 100%, 6.25% (beam width 3.9 msec, 16 times/sec)

The higher current settings were not used due to power restrictions or operational constraints. The 13 mA, 3 kV, 100% mode was locked out due to power limitations and currents above 1 mA were not routinely used due to the detrimental effect the beam had on other instrumentation (Gussenhoven, et al, 1987). Specifically, severe arcing was noted on the satellite surfaces and resulted in the failure of two of the experiments on 29 March 1979 (Koons and Cohen, 1982).

C. SC10/SC-1 DETECTORS

1. Associated Detectors

The SC-1 experiment measured VLF and HF emissions and provided the broadband data presented in the spectrograms. The SC-1 experiment employed two antennas, one for electric field measurements and one for magnetic

field measurements. The electric antenna was a 100 meter tip to tip dipole from the SC10 experiment. The two halves were extended perpendicular to the spin axis. The inner 30 meters of each 50 meter segment was coated with Kapton insulation. The magnetic antenna was an air core loop electrostatically shielded with an effective 575 m^2 cross section at 1.6 kHz mounted on a two meter boom off the belly band of the satellite. The sensitivity of the magnetic receiver was 3×10^{-6} gamma/$Hz^{1/2}$ at 1.3 Hz with a 60 dB dynamic range. The electric field receiver sensitivity was 5×10^{-7} $V/(MHz)^{1/2}$ at 1.3 kHz and 10^{-7} $V/(MHz)^{1/2}$ at 10.5 kHz. The broadband data from these antennas were normally taken for one to two hours each day and when active charge control experiments were in progress. (Fennell, 1982)

III. OBSERVATIONS

A. 20 JULY 1979 2241-2330 UT

Plasma wave data from this period was analyzed to determine the effect the electron gun had on the plasma and/or satellite. Our first example will show: (a) stimulated emissions at the electron cyclotron frequency, and (b) linkage between the stimulated emissions and the gun operation. This example was the most physically interesting set of observations.

The gun operations during this period were designed to study enhanced fluxes of electrons above the beam energy noted in earlier experiments. The gun on-time is clearly evident in Figure IIIA-1 denoted by the change in amplitude of the electric and magnetic field strengths. The strength of the signal in the magnetic data will be shown to play an important role in explaining the data below. This period has been discussed previously by Olsen (1987).

This was a magnetically disturbed day with KP=4 for the 2100-2400 period. The satellite was in the dusk bulge at 7.5 RE, L=8.1 and magnetic latitude of 6 degrees. Figure IIIA-2 shows typical plasma wave data in

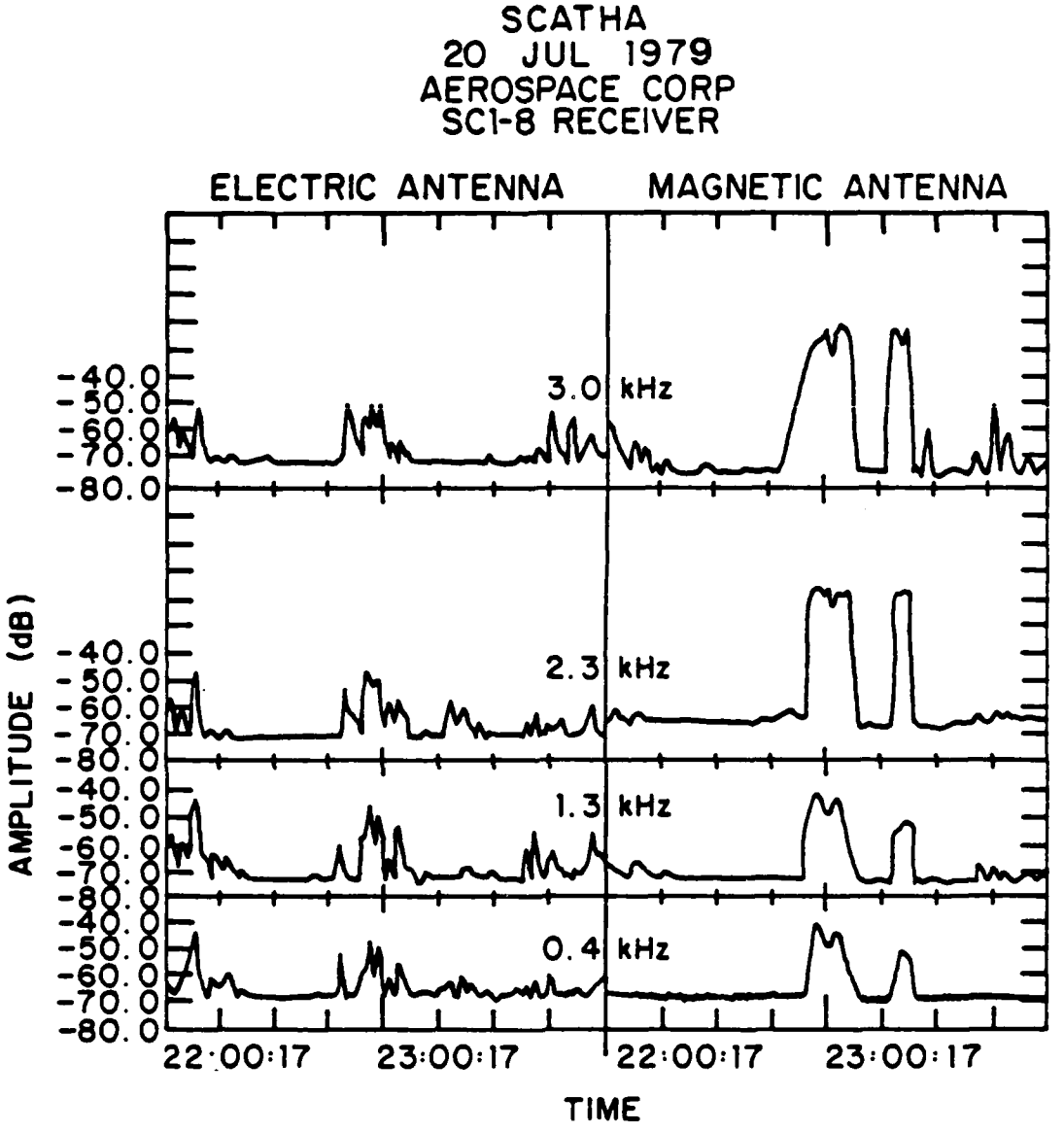

Figure IIIA-1. Narrowband electric and magnetic receiver data for 20 July 1979.

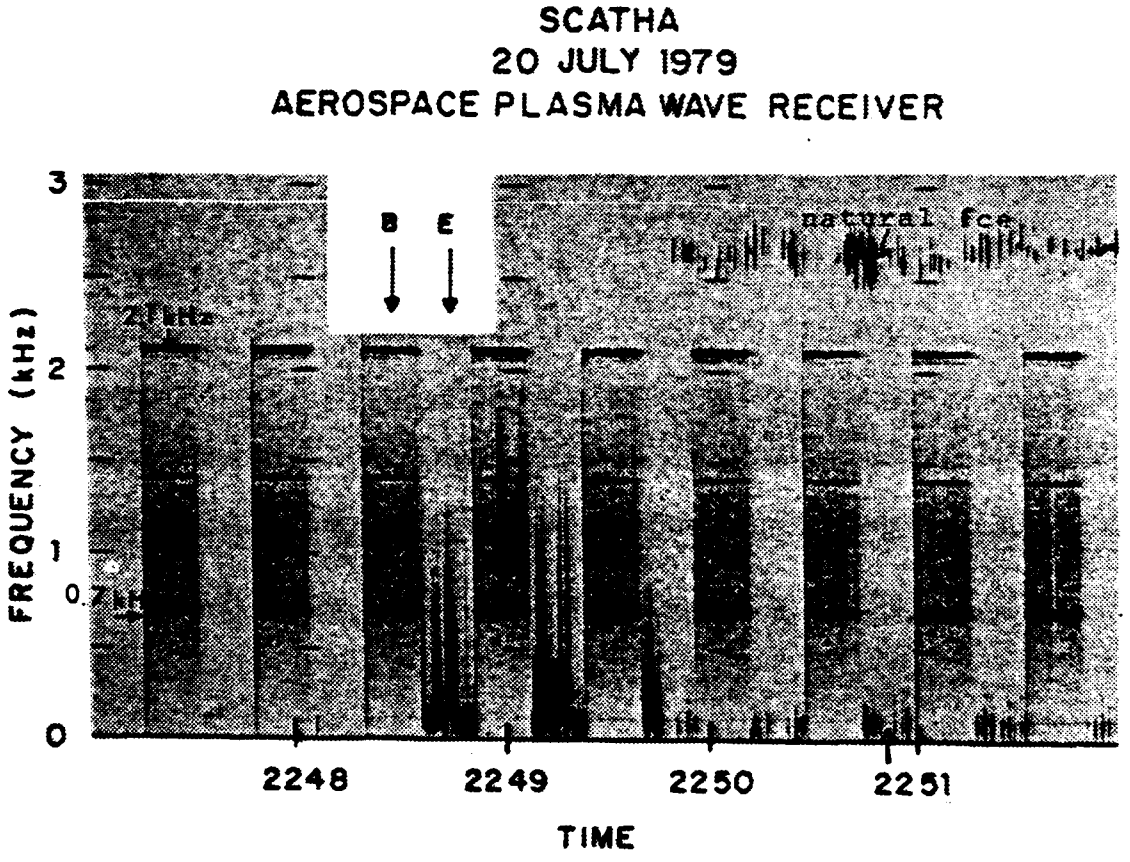

Figure IIIA-2. Spectrogram showing typical plasma wave data. (The arrow indicates the time for the line plot).

spectrogram form for this time period. A spectrogram is a grey scale presentation of the radio data, as a function of time and frequency. The vertical axis is frequency from 0 to 3 kHz. The horizontal axis is time. Amplitude of the signal in DB is proportional to the intensity. High amplitude is plotted as black, low amplitude as white, and intermediate values appear as various shades of grey. For example, intense signals can be seen at 0.7 and 2.1 kHz in the magnetic antenna data, denoted by B, in Figure IIIA-2. The relationship between the spectrogram format and the traditional line plot can be seen by comparing Figure IIIA-3. Figure IIIA-3 is an amplitude versus frequency plot of the data taken at 22:50:50 (indicated by the arrow in Figure IIIA-2). The receiver is cycled between the electric (denoted by the E in Figure IIIA-2) and magnetic antennae (denoted by B) every 16 seconds. Naturally occurring electrostatic electron cyclotron (fce) waves (the short vertical striations between 2250 and 2252) are observed from about 2.5-2.7 kHz. They are identified by the fact that they occur at the unique frequency, fce, as calculated from the magnetic field data. At 22:50:50 this fce frequency was measured at 2590 Hz (Figure IIIA-3). In Figure IIIA-2 strong interference lines are seen in the magnetic

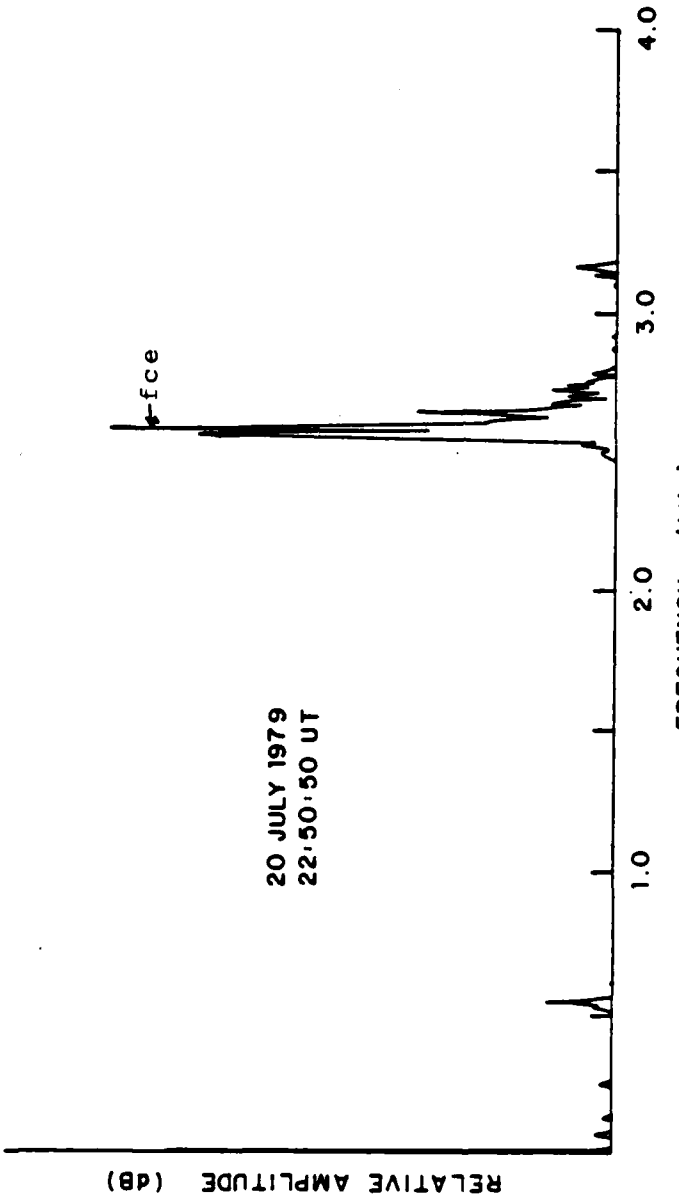

Figure IIIA-3. Electron gyrofrequency measured at 2590 Hz at 22:50:50.

receiver data at 700, 1400 and 2100 Hz. These interference lines are caused by a 700 Hz tuning fork oscillator that is part of another satellite experiment. These interference lines have been identified previously and have been seen in most data. They are highlighted here for identification purposes (Koons, et al, 1982). From 22:48:30 to 22:50:00 (Figure IIIA-2) low frequency (less than 300 Hz) signals can be seen in the electric field data. These appear to be naturally occurring signals since they have finite bandwidth. They have not been identified, however. (Note crosstalk-electrostatic emissions are often observed in the magnetic receiver data. It is likely that the signals we are observing are electrostatic (Koons, et al, 1985; Koons, private communication, 1987). A summary of the SC4-1 commands is listed in Table II.

All the remaining data from this operation is ordered by fce, and we use the measured magnetic field strength from the fluxgate magnetometer to compute and plot fce over the spectra. The electron gyrofrequency was computed from the local magnetic field measured by the magnetometer:

$$fce = eB/6.28m$$

where e is the electron charge (1.602×10^{-19}eV), m is the mass of the electron (9.11×10^{-31} kg), and B is the magnetic field intensity in gammas. The magnetometer accuracy is estimated to be 1 nT at one sigma confidence level on the worst axis (Koons, et al, 1985). Evidence of the magnetic activity can be seen early in the 2241-2330 period in the fluctuation of the magnetic field strength. The naturally occurring electron cyclotron waves (fce) which begin in Figure IIIA-2 at 2250 continue on the next spectrogram (Figure IIIA-4). The naturally occurring waves from 2252 to 2254 (faint vertical stripes) are neatly matched to the calculated time varying gyrofrequency overplotted. The gyrofrequency was computed at 2 second intervals from the magnetic field strength and plotted on the spectrograms (small dots). These waves are similar in appearance with those which will be induced by the electron gun operations.

At 22:52:40 the electron gun system is initialized, and it is powered up at 22:54:54. At 22:55:00 the electron gun is turned on. A prompt, if muddled, effect can be seen on the plasma wave data (Figure IIIA-4). The tuning fork related interference lines are masked and a strong broadband signal can be seen in the magnetic field spectrum. At 22:55:37 the electron beam is energized at

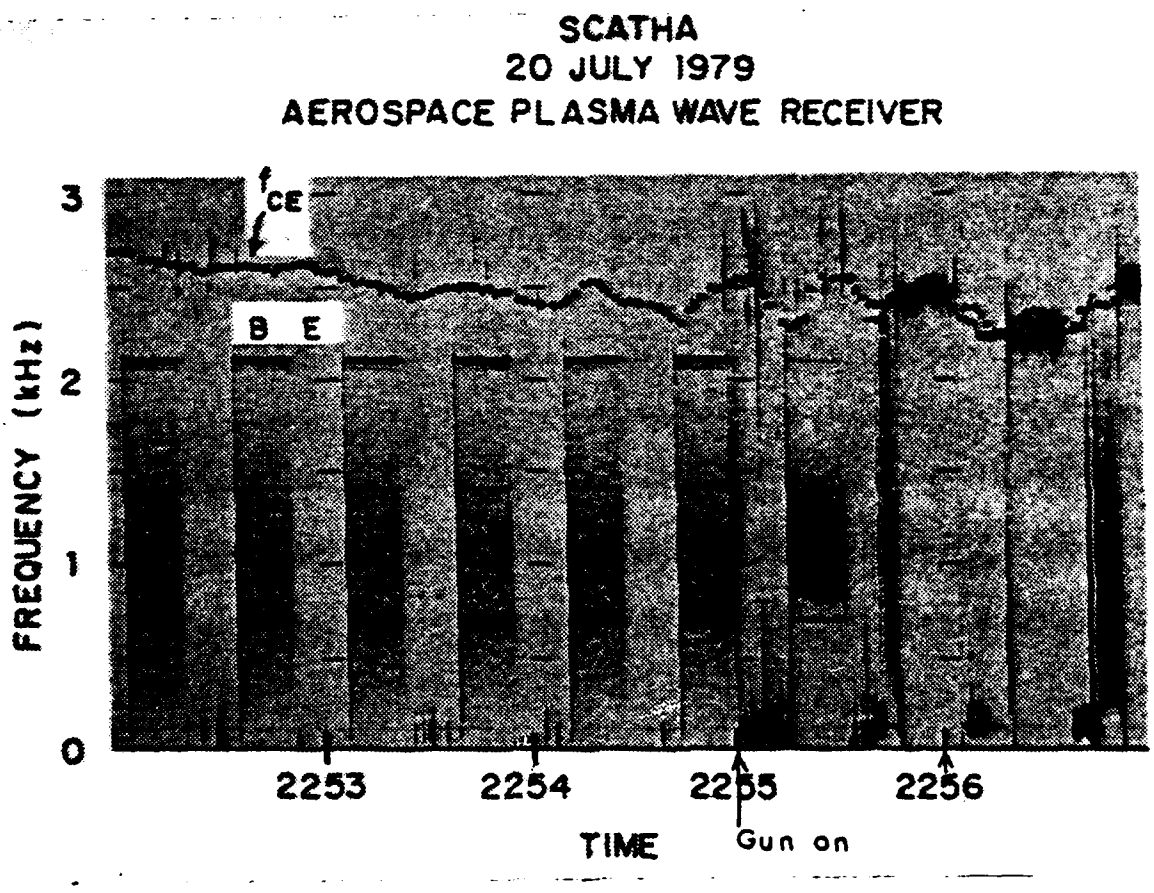

Figure IIIA-4. Naturally occurring electron cyclotron waves are present. Effect of electron gun being turned on is seen at 22:55:00 (arrow). (The second arrow indicates the time of the line plot).

a current level of 10 μA and 50 eV. The gun was operated continuously in this mode until 23:02:28 when the beam current was increased to 100 μA.

A monochromatic signal, similar to the fce wave, is observed in the VLF data during the entire period with the gun on in the 10 μA mode. The intense, monochromatic signal above 2 kHz varied in frequency from about 2400 to 2600 Hz as seen in the latter period of Figure IIIA-4. This signal is modulated in frequency at the satellite spin period of 59 sec, has a very narrow bandwidth, and appears monochromatic in the electric data to within receiver resolution. Figure IIIA-5 is a line plot of magnetic antenna data taken at 22:56:00 (time indicated by arrow in Figure IIIA-4). The only signal seen in this plot is the strong, monochromatic signal near 2400 Hz. The gyrofrequency calculated from the magnetic field strength for this time was 2385 Hz. In the early part of the period after the electron gun was first turned on (22:55:00 - 22:57:00) the signal was at or near the electron gyrofrequency, mimicking the naturally occurring waves.

Figure IIIA-6 shows that significant differences between fce and the signal frequency begin to occur by 22:58:00. In particular, the signal frequency drops

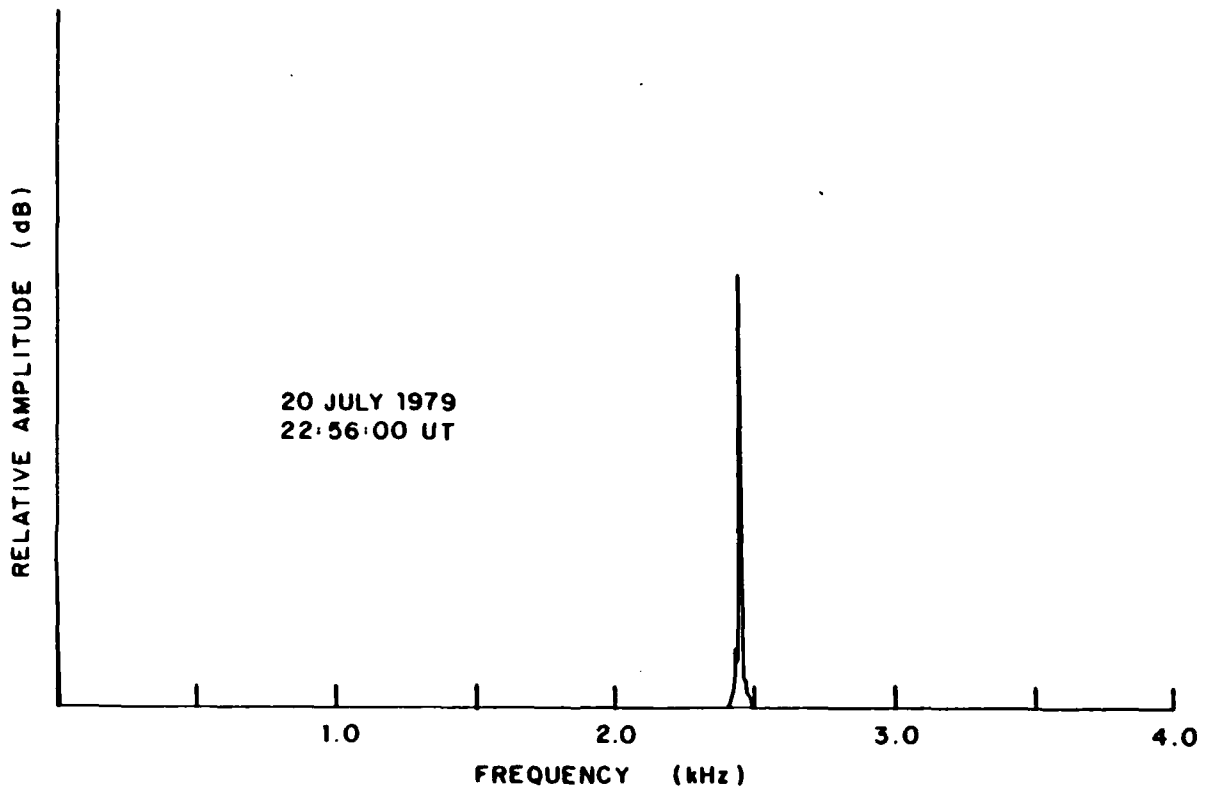

Figure IIIA-5. Monochromatic signal similar to the fce wave seen in the plasma wave data.

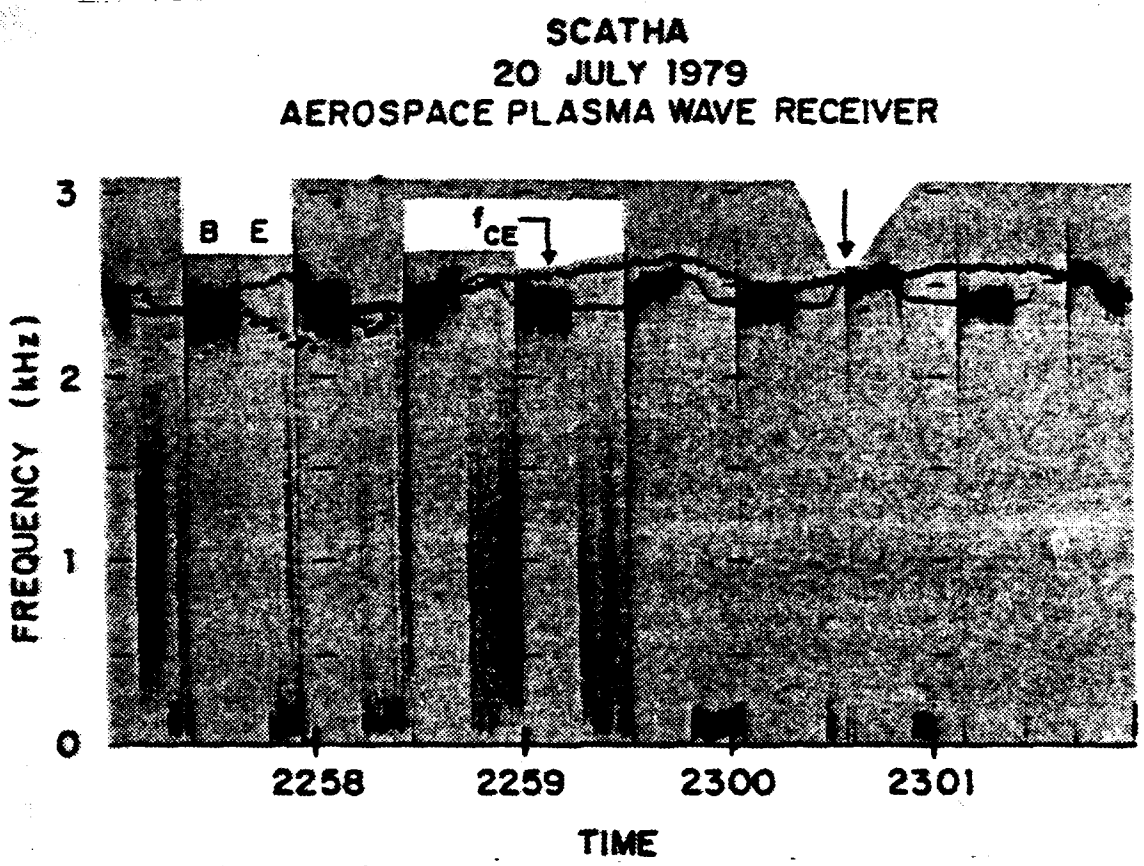

Figure IIIA-6. Spectrogram for 22:57 to 23:02. The monochromatic signal drops below the gyrofrequency at 22:59:00.

substantially below the gyrofrequency (at 22:59:00). This is significant because it suggests the signal is not an electron cyclotron wave. The signal continues for as long as the electron gun is operated in the 10 μA mode. The fluctuation in the frequency of the signal is approximately sinusoidal and is repeatable over several periods. This period is close to or equal to the satellite spin period (Note the location of the 'knee' (at 23:00:30, arrow in Figure IIIA-6) in the electric field spectrogram. This is a distinguishable characteristic of the signal and appears in the same general position on the waveform).

The effect of changing the gun parameters is considered next. A significant change in the plasma wave data will result from a change to the gun parameters. From 23:02:28 to 23:03:15 the gun beam current was increased to 100 μA (Figure IIIA-7). The VLF data with the gun on at 100 μA appeared similar to the data with the electron beam off. The strong interference lines at 700 and 2100 Hz reappear in the magnetic channel. Close examination of the data shows that some of the sporadic naturally occurring electron cyclotron waves are present (but not clearly visible in the figure). The intense

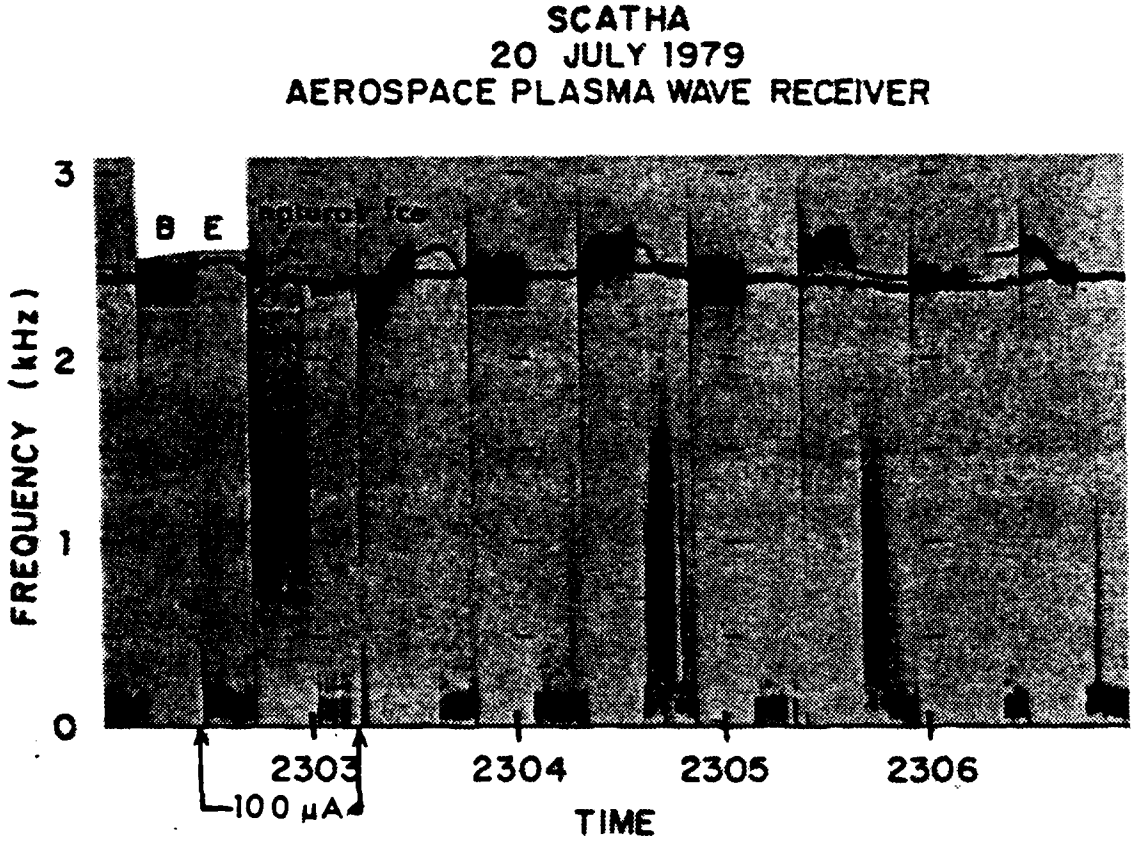

Figure IIIA-7. Spectrogram shows spectra with the electron gun on at 10 μA, 50 volts. Gun current was briefly increased to 100 μA between 23:02:28 to 23:03:15.

monochromatic signal seen at 10 μA beam current disappears.

The repeatability of the monochromatic signal seen previously is shown by returning the gun parameters to 10 μA, 50 volts. At 23:03:15 (in Figure IIIA-7) the beam current was reduced to 10 μA and the VLF characteristics returned to those previously observed at 10 μA beam current (i.e. the 2.4-2.7 kHz signal is again present). The system remained in this configuration until 23:07:41 when the electron beam was turned off (Figure IIIA-8). The VLF characteristics revert to those observed prior to the gun operations (prior to 22:55:00). The 700, 1400 and 2100 Hz interference lines return. For the next 10-12 minutes the electric spectra reveal no obvious signals, and the magnetic antenna shows only the tuning fork lines and receiver noise.

The repeatability of the effects of the electron gun operations are emphasized by repetition of the sequence. At 23:18:31 the electron beam was again turned on at 10 μA beam current. The VLF data (Figure IIIA-9) resume the behavior shown previously. The signal oscillating between 2400-2600 Hz returns and the low frequency signal (100-200 Hz) becomes more intense. From 23:21:34 to 23:21:58 the beam current was increased to 100 μA, and

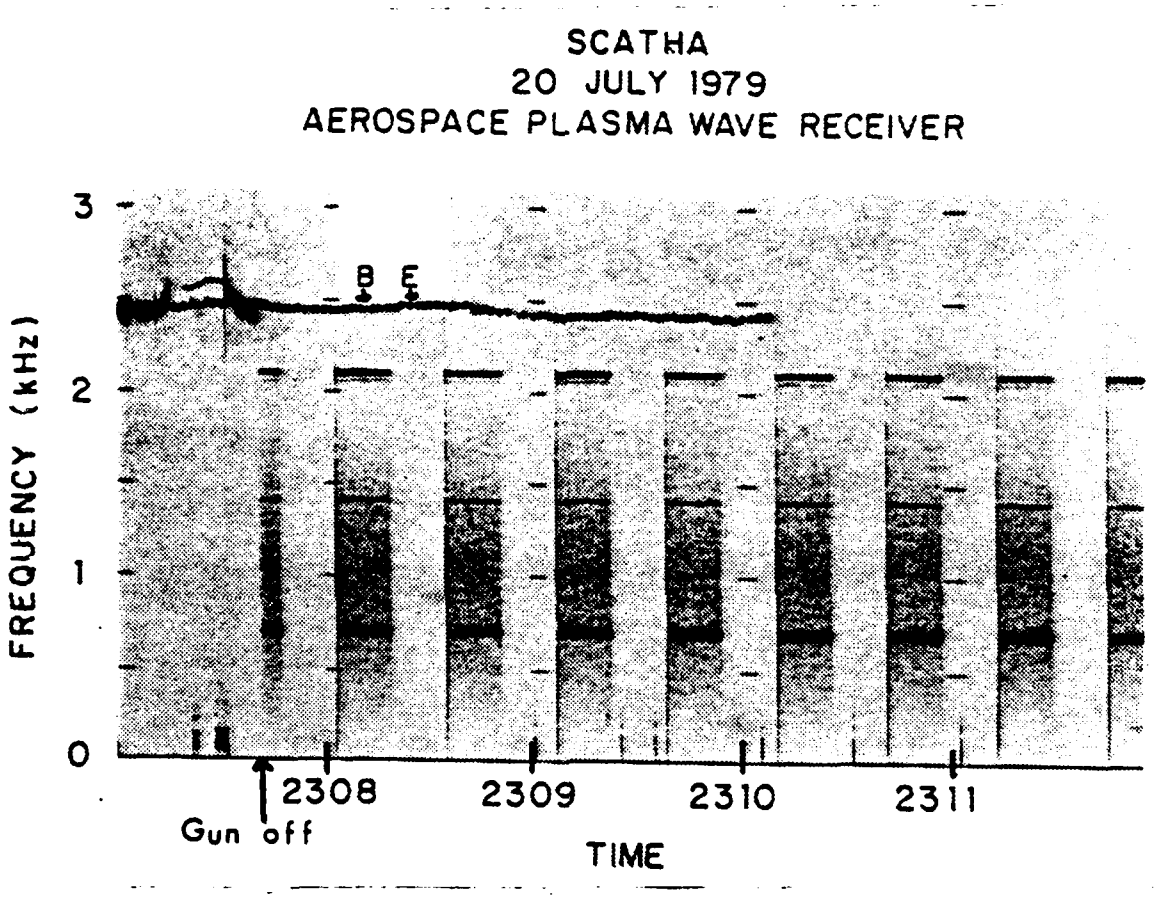

Figure IIIA-8. Spectrogram shows change in plasma wave data when gun was turned off at 23:07:41.

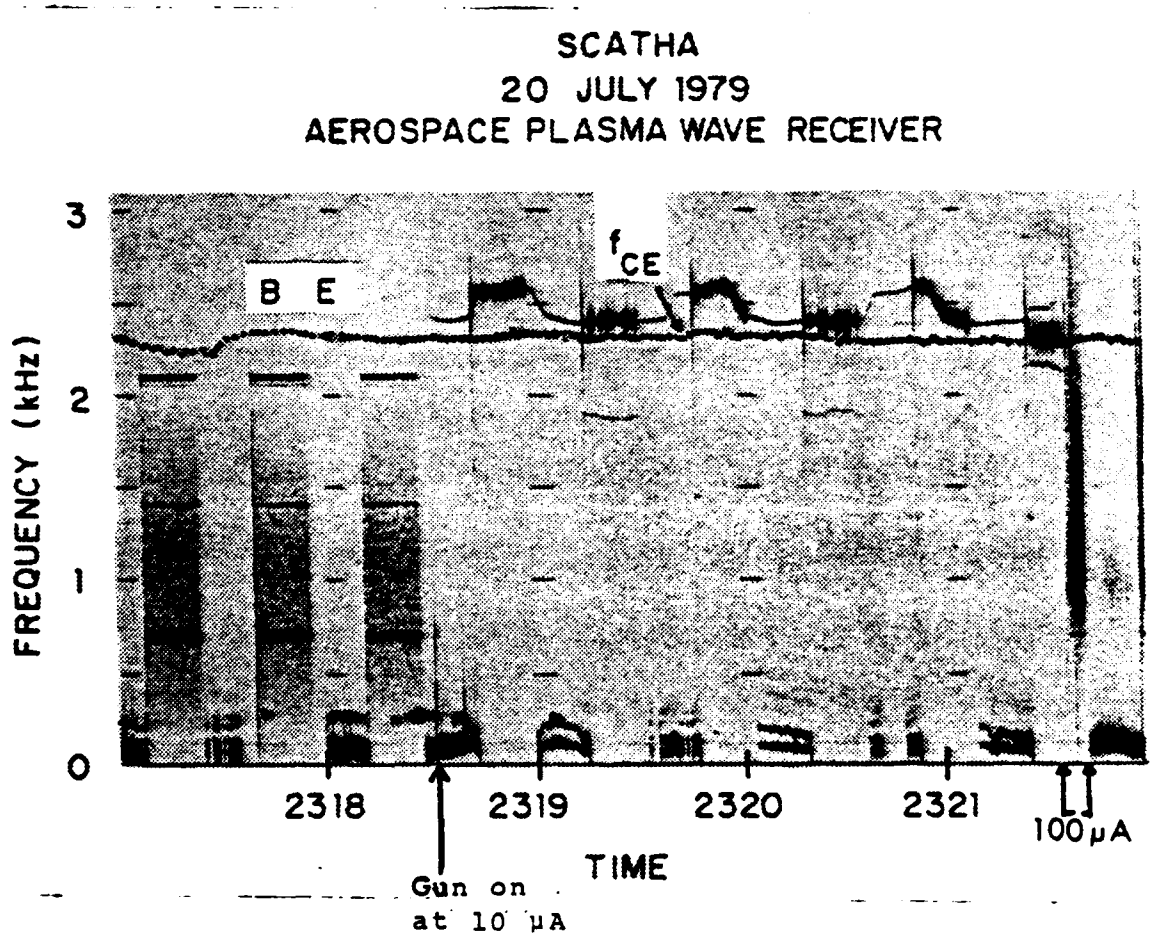

Figure IIIA-9. Repeatability of the effects of the electron gun operation is seen when the beam was reenergized at 23:18:31.

again the 2400-2600 Hz signal disappears and the interference lines reappear in the magnetic data. At 23:21:58 the beam current was reduced to 10 μA and the VLF data regain their now familiar character. At 23:23:48 (Figure IIIA-10) the electron beam was turned off and the 700, 1400 and 2100 Hz interference lines could again be seen in the magnetic receiver data. Also sporadic electron gyrofrequency emissions were present (Figure IIIA-11). During the last period the gun was operated at 10 μA several signals can be seen in the magnetic receiver data (e.g. circled arrow at 23:22:30 in Figure IIIA-10) that are strongly suggestive of an intermodulation effect in the 2.4-2.7 kHz line.

The 2.4-2.7 kHz signal that is observed during the 10 μA mode of operation is strongly linked in frequency characteristics to electron cyclotron waves, near but not at the natural cyclotron frequency. This signal is the dominant effect that was seen in the VLF data during this gun operation and we attempt here to explain the source of this apparently stimulated electron cyclotron wave. The apparent broadness of the signal in the magnetic field data is a result of the AGC control on the satellite and the processing system. Although this signal appears to have a finite bandwidth, it is most

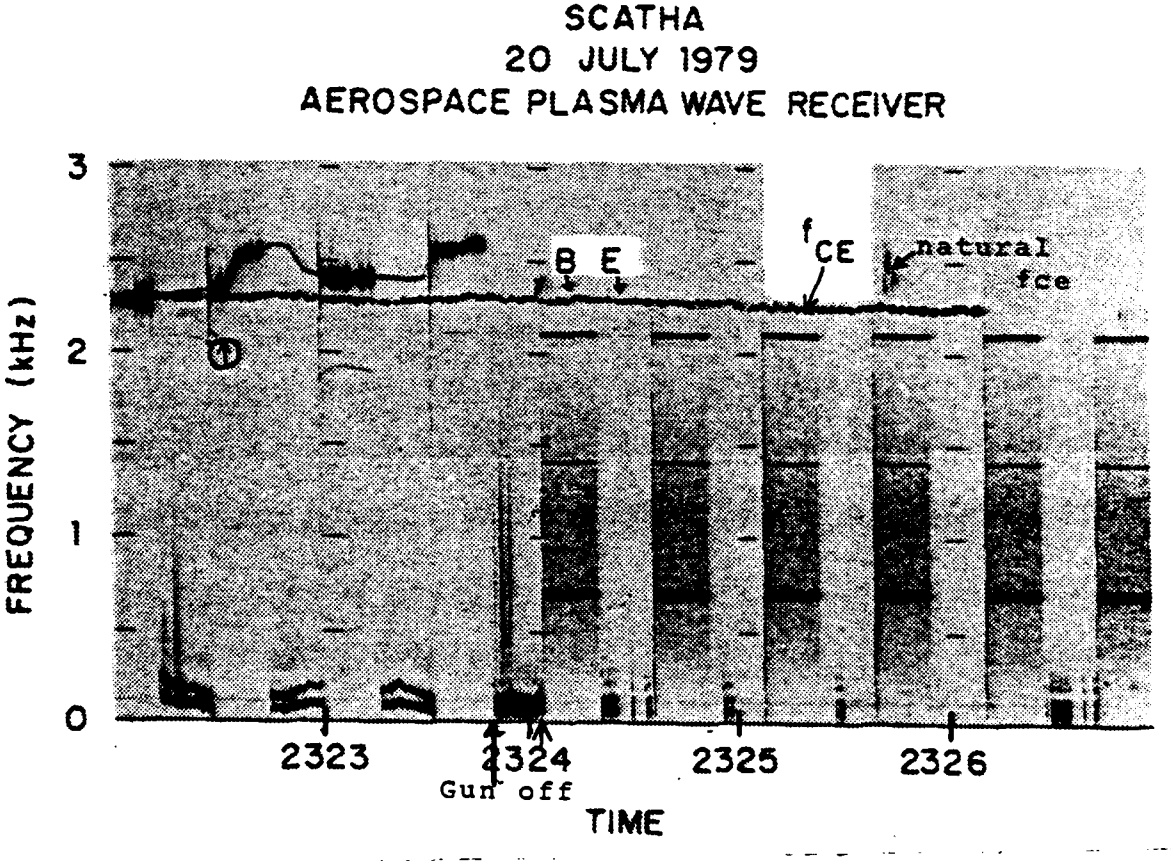

Figure IIIA-10. Electron beam is turned off of 23:23:48. The interference lines at 700,1400 and 2100 Hz return. (The arrow indicates the time of the line plot).

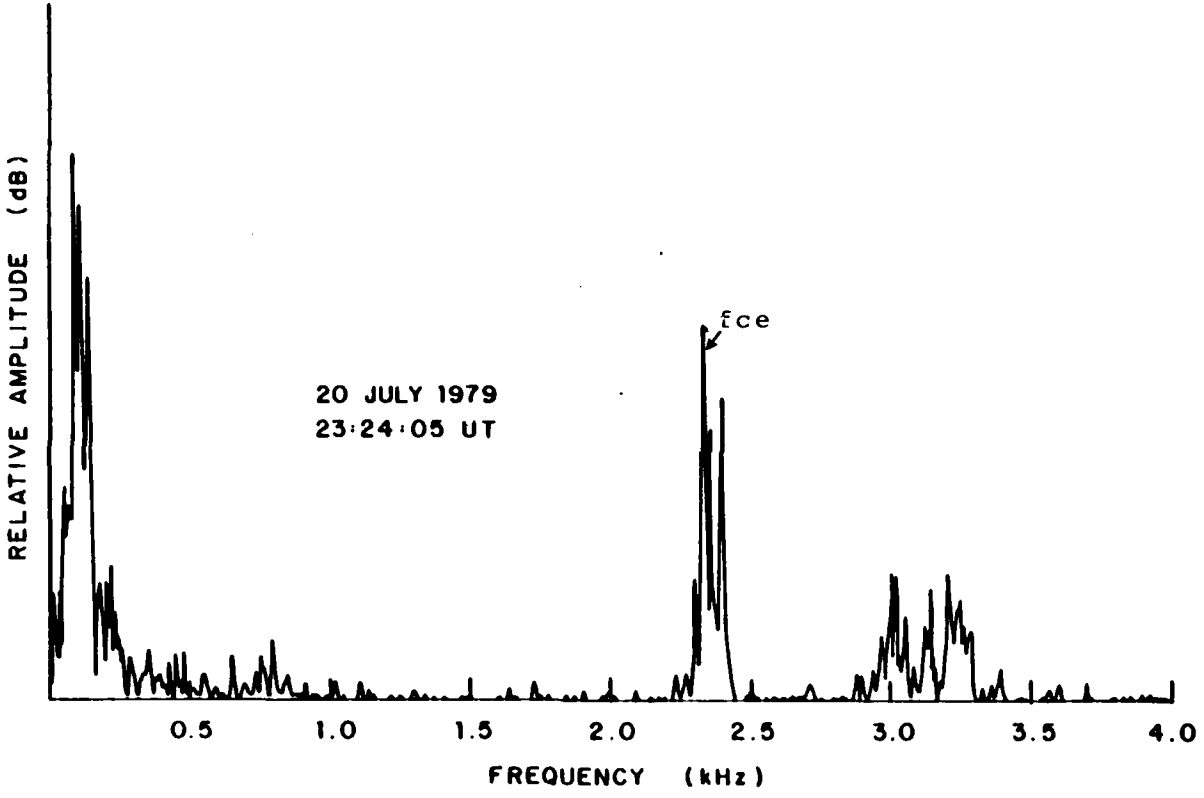

Figure IIIA-11. Sporadic electron gyrofrequency emissions present in the electric receiver data; electron gun is off.

likely the same monochromatic signal observed by the electric antenna. The relatively constant amplitude suggests that the satellite itself is the source of the signal. Since the signal is only visible at 10 μA beam current, there are apparently beam-plasma effects which determine the propagation of the signal to the electric and magnetic antennas through the ambient plasma. Theory holds that there should be no signals below the gyrofrequency due to the dispersion relations. The fact that the oscillation drops below the calculated gyrofrequency is disturbing. Since the signal is close to fce, we pursued the idea that there was something causing the magnetic field strength near the satellite to vary. One thing that might perturb the satellite magnetic field is the solar array current. Figure IIIA-12 is a plot of the solar array current, Isa, for a 305 second period on 19 July 1979. Plotted above the solar array current is the plasma wave oscillation seen on 20 July 1979. The solar array current is obviously modulated at the satellite spin period. This is a result of shadowing of the solar cells as the booms pass between the satellite and the sun. The similarity of the shape of the solar array current to the shape of the plasma oscillation is striking. We suggest that the

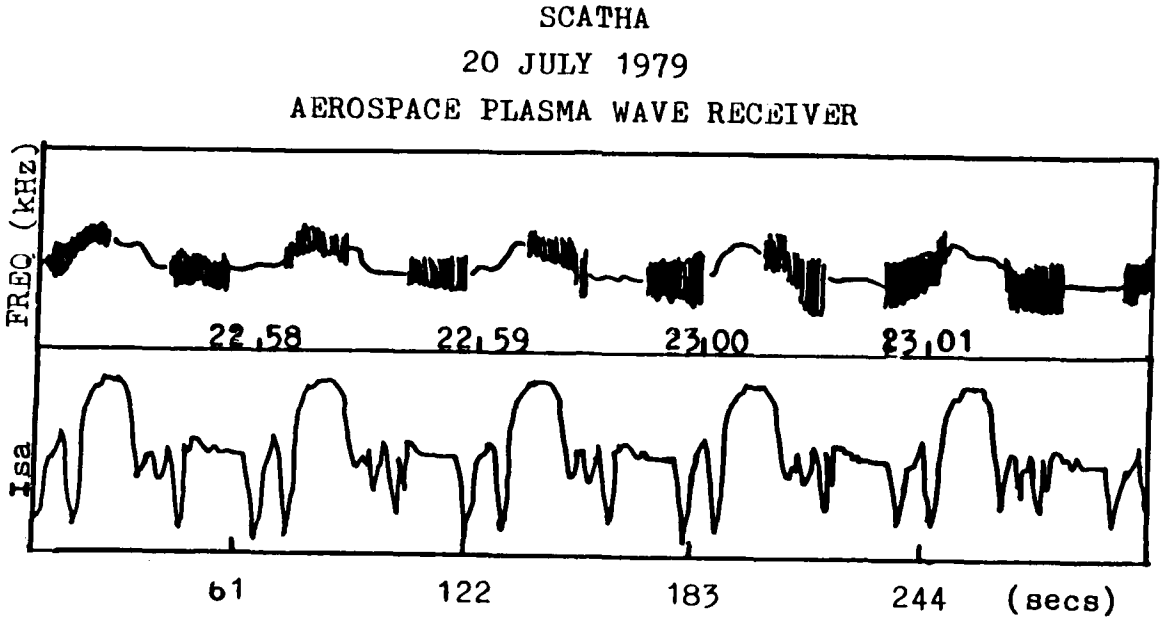

Figure IIIA-12. (top) Plasma wave oscillation with gun on. (bot) Solar array current modulated at the satellite spin period.

solar array current causes a perturbation to the total magnetic field. This field is largely balanced out by design, but is non-zero. The perturbation field, or satellite magnetic moment, will vary with the solar array current, Isa. The perturbation in the magnetic field strength near the satellite then results in a slight change in the electron gyrofrequency. ($\Delta B \propto \Delta Isa$, $\Delta fce \propto \Delta B$).

One explanation as to why the stimulated signals are not at or above the calculated electron gyrofrequency is based on the observations of Isa. The gyrofrequency was calculated from the value of the magnetic field taken from the fluxgate magnetometer which is at the end of a 4 meter boom. The magnetic receiver is at the end of a 2 meter boom and is therefore closer to the satellite surface. The beam itself begins at the satellite surface (0 meters). The perturbation field (e.g. satellite magnetic moment) will be stronger near the satellite. Since the magnetic receiver is closer to the satellite than the magnetometer, it may be responding to a signal at the local electron cyclotron frequency, rather than the frequency determined by the magnetometer. Note that the value of the magnetic field obtained from the magnetometer has an error estimated to be a few gammas

associated with satellite generated fields (B. Ledley, private communication, 1987). This means the perturbation in the magnetic field strength drops to on the order of 1 gamma by 4 meters. The concept of a perturbation field of 1 gamma at 4 meters, 10 gamma at 2 meters and 100 gamma at the satellite surface is consistent with a fluctuation in fce of 280 Hz at 2 meters and a fluctuation in solar array current on the order of 5 A. Assuming that B has a relationship to the perturbed current of the form $B \alpha \mu_o I (R_{SAT}/r)^3$, then the values for the magnetic fields strengths at 2 and 4 meters required for a 200-300 Hz change in fce are correct to within sensor accuracy. This could account for the plasma oscillation appearing below the gyrofrequency. The oscillation varies in frequency by only a few hundred hertz. The magnetic intensity would only have to vary at the loop antenna on the order to 6-7 gamma to produce this change, well within our estimates. Note again that the modulation of the solar array current closely matches the shape of the plasma oscillation (Figure IIIA-12).

The above scenario assumes that the stimulated wave frequency is determined by the local magnetic field strength at the antenna. It also assumed that the

electric antenna couples in close to the satellite. Note in Figure IIIA-9, for example, that when the receiver switches from the magnetic to the electric antenna the frequency of the stimulated wave does not change. This would be the case only if the electric and magnetic antennae coupled at the same radius. Considering the location and size of the antennae this is unlikely. It is possible, instead, that the signal is generated close to the satellite (within first meter) and is being "broadcast" to both antennae. This would explain why no frequency shift is seen when the receiver switches antennae. However, this means the beam interacts with the plasma in a very limited range, near the satellite. Above we assumed a perturbation field near the satellite surface to be approximately 100 gamma to produce a 200-300 Hz frequency shift at 2 meters from the surface. If the beam-plasma interaction is taking place closer to the satellite the strength of the perturbation field would have to be smaller to be consistent with the frequency of oscillation we observe. We assumed the satellite magnetic field varied as $1/r^3$ when, in fact, near the satellite a more complicated, undetermined dependence may be the controlling factor in determining the local magnetic field. Hence, the frequency of any stimulated

wave generated at the point of the beam-plasma interaction would vary depending on the local magnetic field fluctuations.

We observed similar behavior over several operational periods on this day. No other examples of fce related emissions have yet been found on other days. A relationship between the operation of the electron gun and the plasma wave spectra is consistently found. The gun operation either couples satellite (electron gun) generated interference to the plasma wave experiments or the beam interacts with the plasma near the satellite in a characteristic, repeatable way. This latter possibility is suggested by the beam current dependence, and discounted by the relationship to the electron cyclotron frequency. Given the limitations to the accuracy of the sensors (especially the magnetometer) and their location with respect to the satellite, the observation of the stimulated plasma wave below the gyrofrequency can be adequately explained. The mechanism for the generation of the signal has not been pursued, but observations suggest that a plasma wave was stimulated at the electron gyrofrequency due to operation of the electron gun. This would be consistent with

standard calculations of beam generated waves (Chen, 1985).

B. 3 APRIL 1979 14:13:00 - 14:36:36

The initial intent of this thesis was to provide a basis for understanding electron observations which had been interpreted as electron heating. The intense fce wave seen on Day 200 provides such a basis. A second goal was to catalogue the plethora of interference lines that are commonly seen in the plasma wave data so that the remaining features in the data could be identified and understood. Towards that goal this sections provides examples of spectrograms taken during different modes of operation of the electron gun.

The photographs of the spectra taken during the different modes of operation of the electron gun are presented below. The photographs are arranged in a sequence of operations at different gun current and voltages. The lowest current setting is presented first with the corresponding voltages (1 μA; 50, 150, 300, 500, 1500, and 3000 volts). The current is then increased to 10 μA and then to 100 μA and each voltage setting is stepped through in sequence. Common features between similar settings for the electron gun (voltage or

current) are not readily apparent. The only feature that can be considered common is the presence of the interference lines which appear throughout the data with the electron gun on or off. The appearance of the interference lines does not appear to be tied to any particular setting of the electron gun parameters and may most likely be a function of the setting of the automatic gain control of the receiver. The descriptions below will identify those signals that are common interference lines and any particular unique characteristics of the plasma wave data.

The electron gun operations during this period were designed to determine the effect the various gun modes of operation had on the plasma wave data. The satellite was at L7.2, magnetic latitude of -17 degrees and midnight local time. The electron beam was operated over a wide range of energies and currents. The maximum current setting was 100 μA due to the detrimental effects on other instruments on the satellite noted during previous experiments. Gusshoven, et al, (1987) reported the effects of electron gun operations on spacecraft charging during experiments on Day 90, 1979 and Days 312 and 313, 1983 which were similar in nature to the Day 93 experiments. The electron gyrofrequency was near 4.2 kHz

during this time (B. Ledley, Private communications, 1987). A summary of the SC4-1 experiment commands is included in Table III.

The first set of figures show the typical plasma wave characteristics with the gun off. The spectrograms shown are grey scale presentations of the radio data. The vertical axis is frequency from 0-6 kHz. (The vertical axis scale is different from that of the previous spectrograms due to a different receiver mode.) The horizontal axis is time. The amplitude of the signals in DB is proportional to the intensity of the grey scale, white being the lowest amplitude, black being the highest. The signals that are present are those that are related to satellite systems or ambient in the environment. In Figure IIIB-1 the spectrum prior to the SC4-1 power being turned on can be seen. Figure IIIB-2 is the line plot of the magnetic receiver spectra during the time the gun is off. Present in the magnetic field data are the 700 Hz tuning fork and the 1400 and 2100 Hz tuning fork harmonic interference lines. These interference lines were discussed in the Chapter IIIA (Day 200) of this thesis. The 1400 Hz line can only be seen faintly. Also present is an interference line at approximately 3 kHz. Receiver noise characterizes the

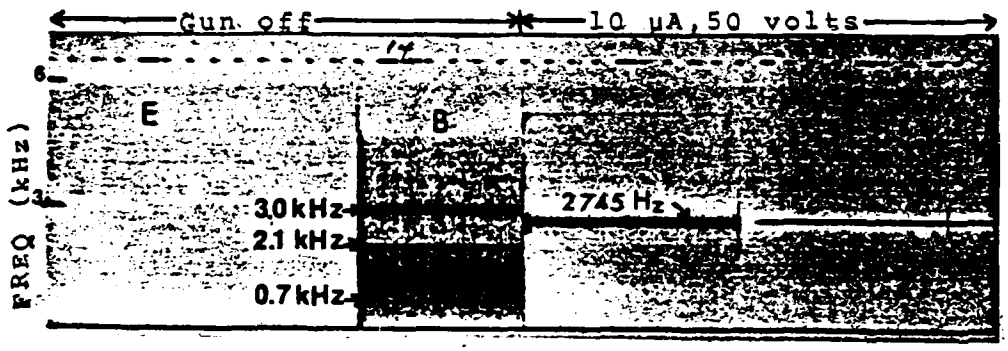

Figure IIIB-1. Beam on at 14:14:04, 10 μA, 50 volts.

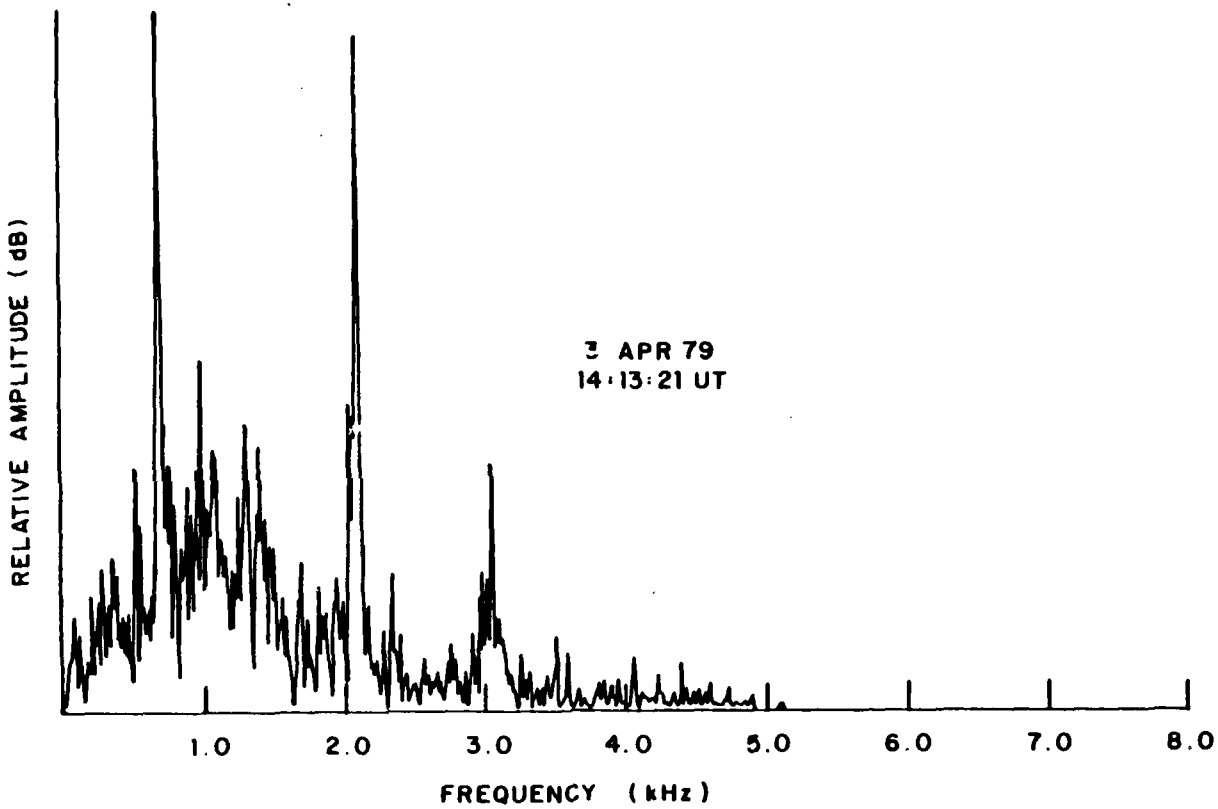

Figure IIIB-2. Magnetic receiver frequency spectrum taken at 14:13:21 on 3 April 1979. Interference lines are present at 700, 1400, 2100 and 3000 Hz. The electron gun is off.

remaining distinctive feature in the spectrogram. These signals are present only in the magnetic receiver data. The electric receiver spectrograms ar essentially void of any signals. Apparently these interference lines are being generated by other experiments on the satellite. The signal strength is probably low which would explain their absence in the electric data. Turning on the electron gun system power at 14:13:34 did not affect the characteristic of the plasma wave data.

Returning to Figure IIIB-1, there was an immediate effect on the plasma wave data when the electron beam was activated at 14:14:04 at 10 μA, 50 volts. The tuning fork interference lines are masked and another signal at 2745 Hz (measured on spectrum analyzer) appears. This frequency is well below the electron gyrofrequency for this period. This signal appears to have approximately a 300 Hz bandwidth in the magnetic receiver data, but appears monochromatic in the electric field data. The signal is probably monochromatic in both receivers and is being "smeared" in the magnetic receiver data due to receiver gain.

Figure IIIB-3 shows the changes to the plasma wave data as the beam parameters are stepped through the 1 μA; 50, 150 and 300 volt modes. The beam current was reduced

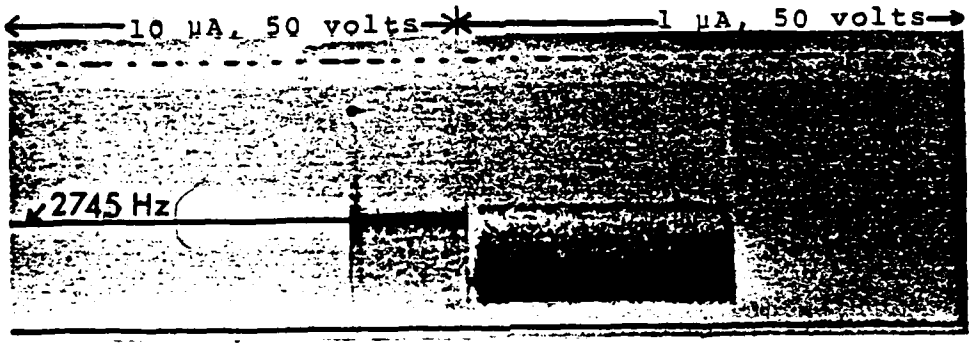

(a) Beam to 1 μA, 50 volts at 14:14:34.

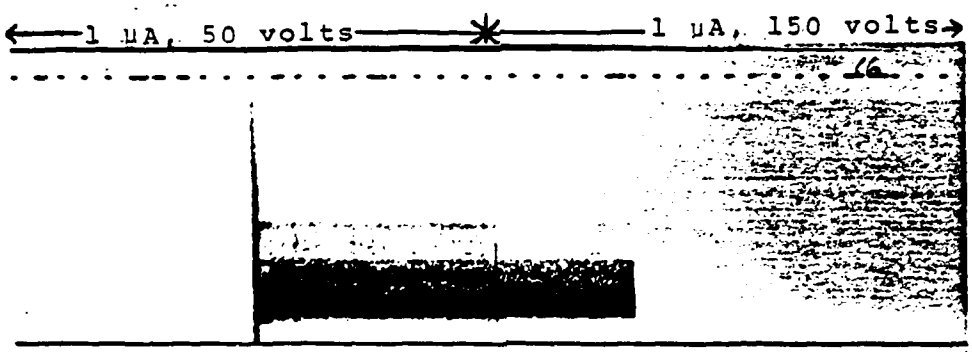

(b) Beam to 1 μA, 150 volts at 14:15:43.

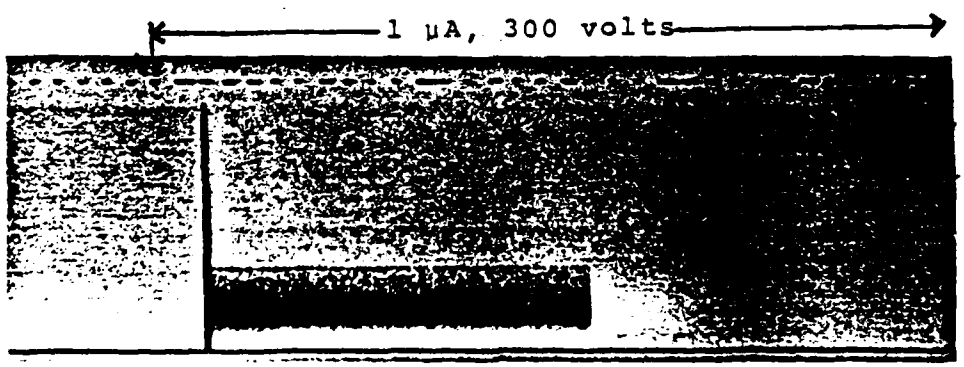

(c) Beam to 1 μA, 300 volts at 14:17:09.

Figure IIIB-3. Spectrograms for beam current of 1 μA; 50, 150 and 300 volts.

to 1 μA at 14:14:34 (Figure IIIB-3a). Broadband receiver noise between 500-2500 Hz is present in the magnetic data. No signals are seen in the electric data and the tuning fork and the 3 kHz interference line is masked. The beam energy is increased to 150 volts at 14:15:43 (Figure IIIB-3b). A broadband signal from 700-2100 Hz is the cominant feature in the magnetic data. The electric data is essentially featureless. The beam energy is increased to 300 volts at 14:17:09 (Figure IIIB-3c). The plasma wave characteristics are essentially the same as those at 150 volts.

Figure IIIB-4 shows the change in the characteristics of the plasma wave data as the gun is stepped through the 1 μA; 500, 1500 and 3000 volt modes. The beam energy is increased to 500 volts at 14:18:19 (Figure IIIB-4a). Figure IIIB-5 shows the line plot of the magnetic receiver data at the 1 μA, 500 volts setting. The 700 Hz tuning fork interference line is very strong and the 2100 Hz and the 3 kHz lines can be seen faintly. Receiver noise dominates the rest of the spectrum and is strongest around 1 kHz. Returning to Figure IIIB-4a, it can be seen that the interference lines are more evident after the mode change. When the beam energy is increased to 1500 volts, Figure IIIB-4b shows no significant change to

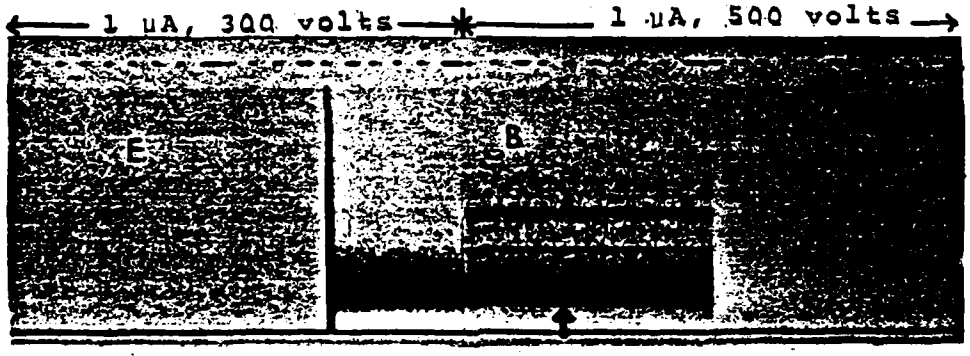

(a) Beam to 1 μA, 500 volts at 14:18:19.

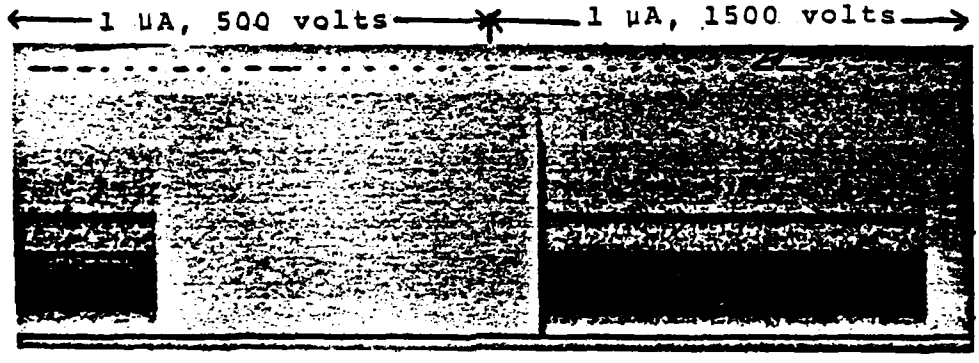

(b) Beam to 1 μA, 1500 volts at 14:19:44.

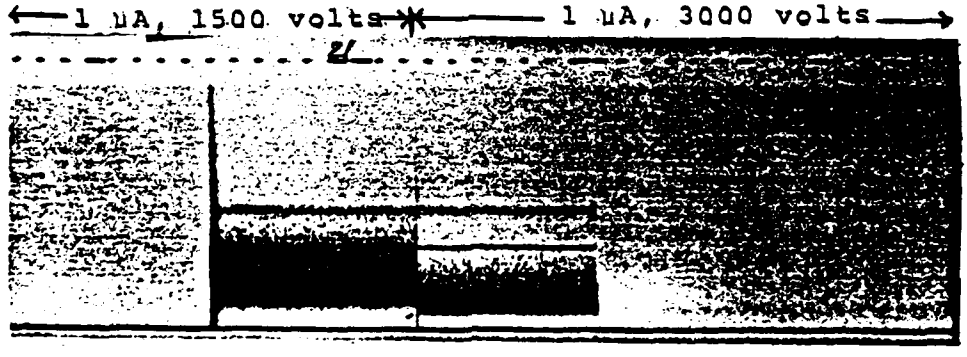

(c) Beam to 1 μA, 3000 volts at 14:21:02.

Figure IIIB-4. Spectrograms for beam current of 1 μA; 500, 1500 and 3000 volts. (Arrow indicates time of line plot).

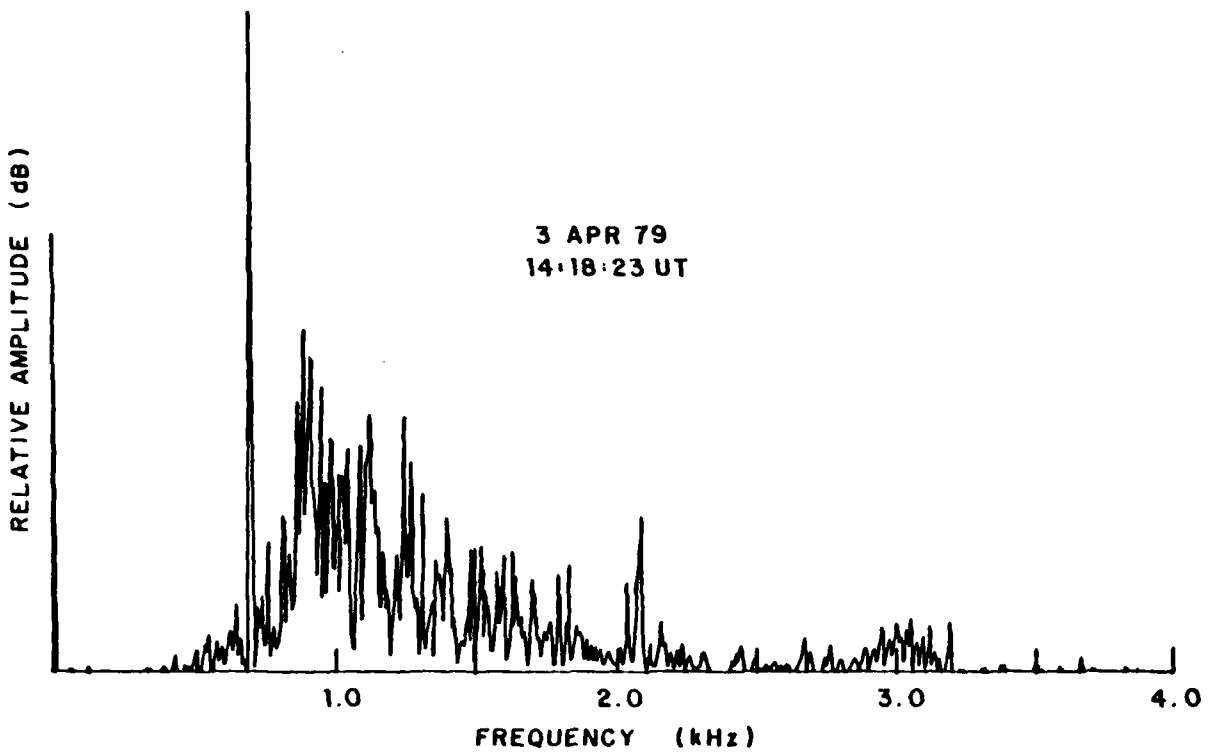

Figure IIIB-5. Magnetic receiver spectrum with electron beam on at 1 μA, 500 volts. The 700 and 2100 Hz tuning fork interference lines are the most prominant features.

the plasma wave data. When the beam energy is increased to 3000 volts at 14:21:02 (Figure IIIB-4c), the lower limit of the broadband signal seen in the magnetic data shifts down in frequency from about 700 Hz to about 500 Hz and the 2100 Hz tuning fork line is more distinct.

The 1 μA beam operations did not result in any gun specific interference lines. The reception of the 700/2100 Hz tuning fork lines, and 3 kHz satellite line were affected, presumably by modification of the satellite AGC. This is consistent with our expectations, since 1 μA is less than the naturally occurring photoemission current, ambient electron current, and secondary emission current by a substantial fraction (1-10%). The next current level up, 10 μA, is comparable to the natural currents, and will perturb the satellite system substantially.

Figure IIIB-6 shows the effect the gun operations had at 10 μA on the plasma wave data. Figure IIIB-6 shows the plasma wave data while the gun was operated in the 10 μA; 50, 150 and 300 volt modes. A substantial variety of new interference lines are found. Koons (private communication, 1987) suggested that a voltage controlled oscillator that is part of SC4 or another experiment may be responsible for some of the interference lines

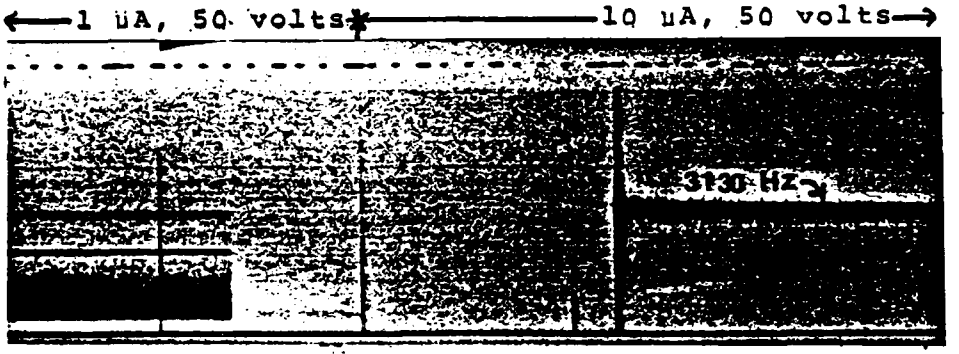

(a) Beam to 10 μA, 50 volts at 14:22:27.

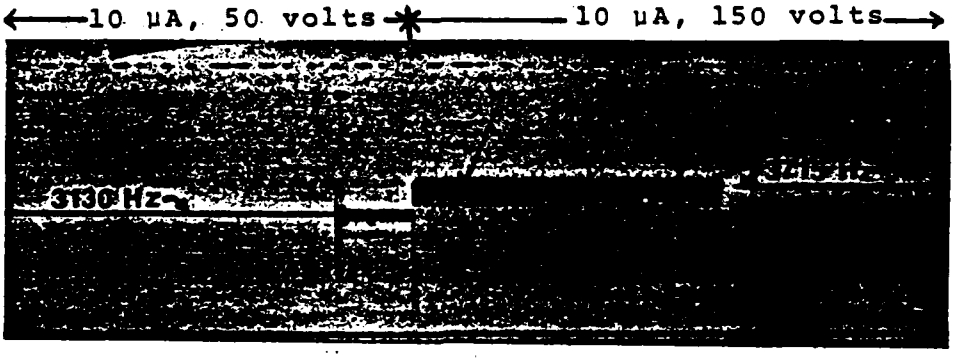

(b) Beam to 10 μA, 150 volts at 14:23:36.

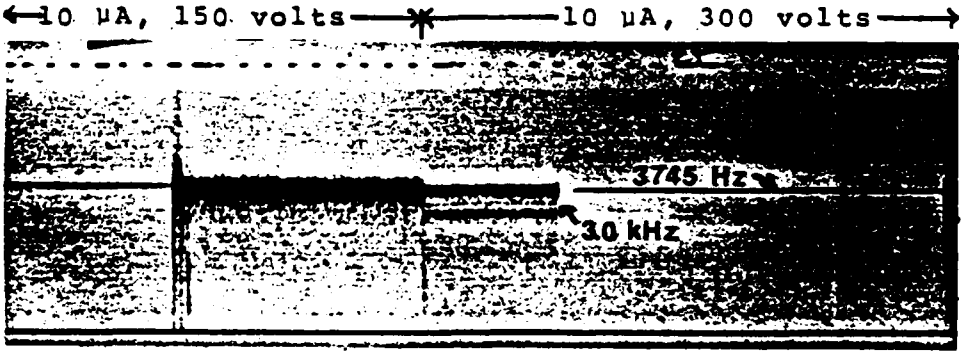

(c) Beam to 10 μA, 300 volts at 14:24:47.

Figure IIIB-6. Spectrograms for beam current of 10 μA; 50, 150 and 300 volts.

observed. There is some evidence in the data of Figure IIIB-6 that tends to support this contention. The beam voltage is reduced to 50 volts and at 14:22:27 the beam current is increased to 10 μA (Figure IIIB-6a). The 700 Hz and 2100 Hz interference lines seen previously are masked and a strong signal at 3130 Hz appears in the magnetic and electric data. This signal at first appeared to be the 3 kHz interference line, shifted in frequency. It is shown below, however, that the "3 kHz" line is separate and distinct. At 14:23:36 the beam energy is increased to 150 volts (Figure IIIB-6b). A signal now appears in the magnetic data at 3715 Hz. This signal is broadband (approximately a 500 Hz bandwidth) in the magnetic and monochromatic in the electric data. This difference in width again reflects the difference in receiver gain, but also reflects the proximity of the magnetic antenna to the spacecraft. The satellite potential increases slightly at this point to about 30 volts (Olsen, 1987). This particular signal is unique and is not identifiable with any previously seen signal. It appears to be related to this particular mode setting of the electron gun. The beam energy is increased to 300 volts at 14:24:47 (Figure IIIB-6c) with a corresponding increase in the spacecraft potential. The 3 kHz

interference line is now present along with the 3745 Hz line. This discounts the 3745 Hz line being a variation of the 3 kHz line affected by a voltage controlled oscillator and indeed indicates that the 3 kHz line from the satellite is not varying in frequency. Another unique aspect of the signals seen at 3130, 3715 and 3745 Hz in the 10 μA; 50, 150 and 300 volt modes is that these signals were seen in both the magnetic and electric receiver data, broadband in the magnetic and monochromatic in the electric. The common interference lines previously identified were present only in the magnetic data, and the electric spectra was essentially featureless. Evidently, the signal particular to these modes is much stronger, allowing it to be propagated to the electric antenna. Observations of other SCATHA plasma wave data (not shown) confirmed that this signal appears to be unique to these particular gun parameters.

Figure IIIB-7 shows the plasma wave data for the 10 μA; 500, 1500 and 3000 volt settings. The beam energy is increased to 500 volts at 14:25:58 (Figure IIIB-7a) while the receiver was tuned to the electric antenna. The electric data is still essentially featureless, but a significant change is noted in the magnetic data from the previous mode. When the receiver switches to the

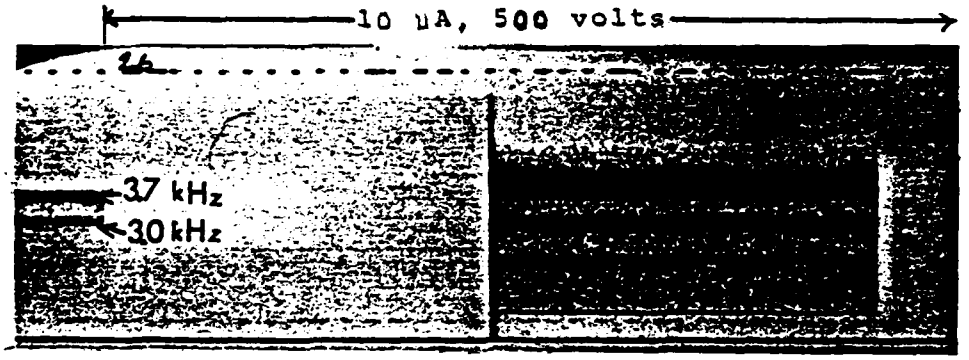

(a) Beam to 10 μA, 500 volts at 14:25:58.

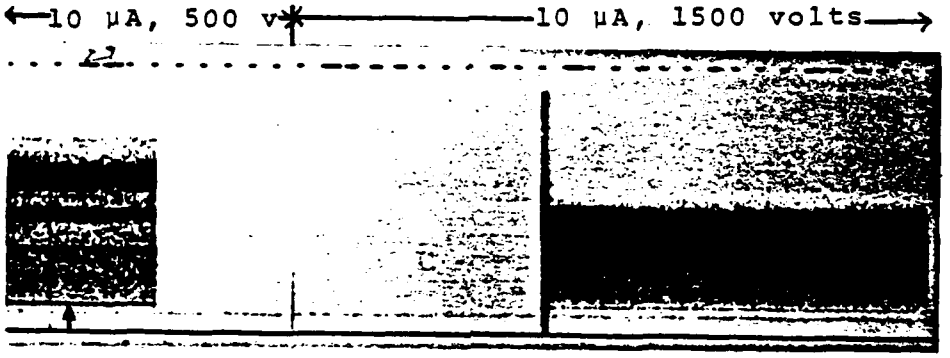

(b) Beam to 10 μA, 1500 volts at 14:27:07.

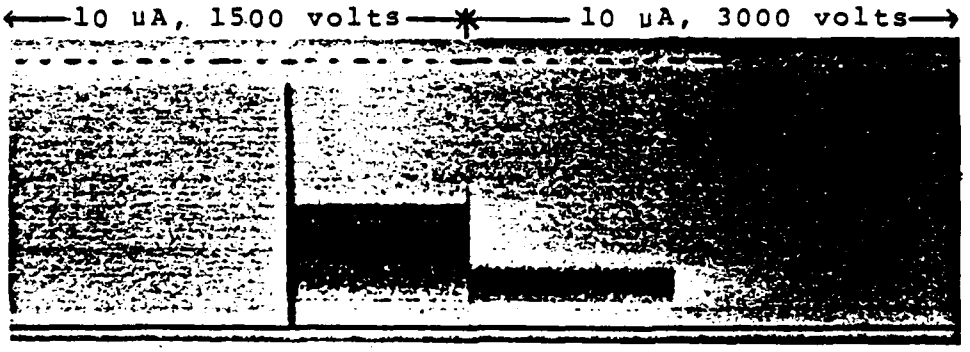

(c) Beam to 10 μA, 3000 volts at 14:28:29.

Figure IIIB-7. Spectrograms for beam current of 10 μA; 500, 1500 and 3000 volts. (Arrow indicates time of line plot).

magnetic antenna the tuning fork and 3 kHz lines are again present. A broadband signal (approximately 1 kHz bandwidth) centered at 4 kHz is also seen. Figure IIIB-8 shows the details of the frequency spectrum for the magnetic data during this time. The tuning fork and 3 kHz lines are clearly seen. The signal at 4 kHz is the most dominant feature. An unknown signal also appears at 5800 Hz. The beam voltage is increased to 1500 volts at 14:27:07 (Figure IIIB-7b) and a broadband signal between 700 and 3100 Hz becomes the main feature in the magnetic spectrogram. The signal seen previously at 4 kHz has disappeared and the 700 Hz and 3 kHz interference lines appear to be lower and upper cutoff frequencies for the signal in the magnetic data. The nature of this signal is characteristic of receiver noise and may be the result of the gain control setting of the receiver. At 14:28:29 (Figure IIIB-7c) the beam energy is increased to 3000 volts. The magnetic receiver noise changes from a 0.5-3 kHz signal to a lower bandwidth centered near 1250 Hz.

The higher voltage (500-3000 V), 10 μA beam experiments resulted in significantly different results than lower voltage settings. The distinction between the two categories exists for two reasons. First, at higher voltage settings, the bulk of the beam probably escapes,

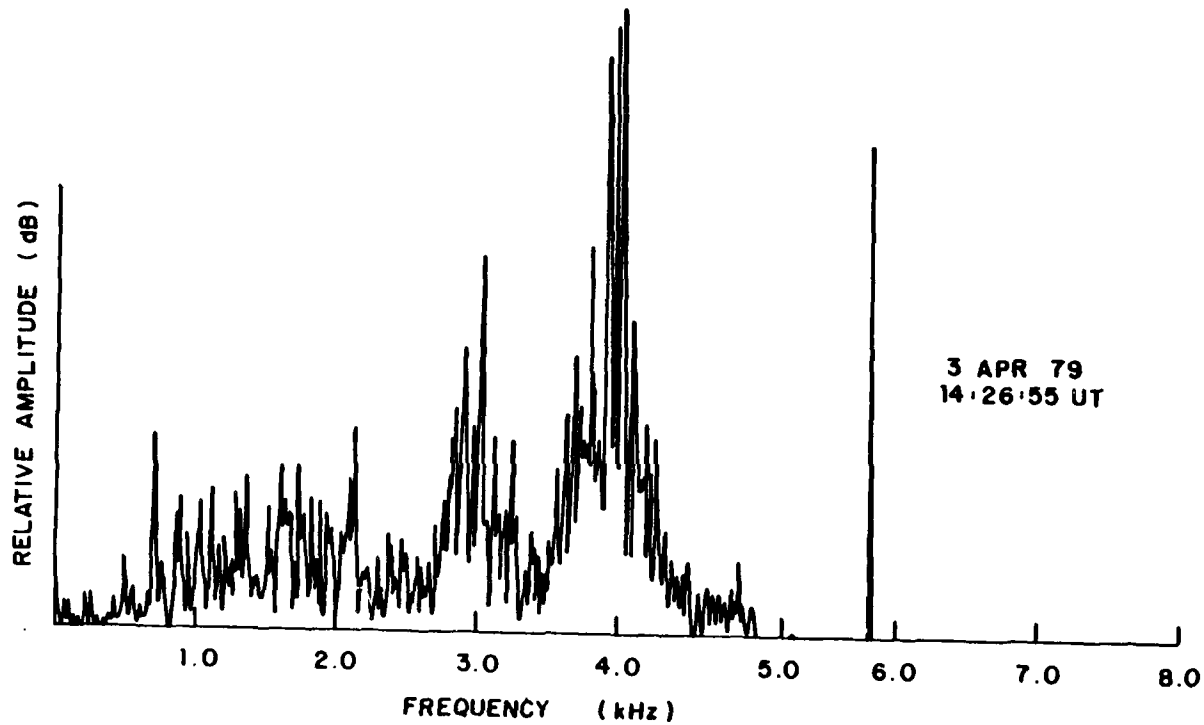

Figure IIIB-8. Spectra taken while receiver is tuned to the magnetic receiver. The beam is on at 10 μA, 500 volts.

since the beam energy is so much larger than induced satellite potentials, (This ignores the possibility of inducing large differential potentials, which apparently does not occur at this time.) Second, since the beam density, current and voltage are related ($I \propto$ Area $\times$ density $\times \sqrt{\text{energy}}$), increasing energy means decreasing density. Hence, the perturbation of the local electron distribution function (bump on tail) becomes less significant, as it moves out the tail, and decreases in magnitude.

Figure IIIB-9 deals with the gun operation in the 100 μA; 50, 150 and 300 volt modes. The beam energy is reduced to 50 volts; the 3.0 and 3.1 kHz lines reappear together. At 14:29:41 (Figure IIIB-9a) the beam current is increased to 100 μA. No interference lines are found at this initial setting. At 14:29:45 faint natural emissions can be seen in the electric field data. At 14:29:59 when the receiver is again tuned to the magnetic antenna a broadband signal is observed. Superimposed on this signal the 700, 2100 and 3000 Hz lines can be distinguished. At 14:30:08 a strong (probably natural) signal at 4480 Hz is seen for approximately 2 seconds in the magnetic antenna data. Figure IIIB-10, which was taken at a slightly earlier time than shown in Figure

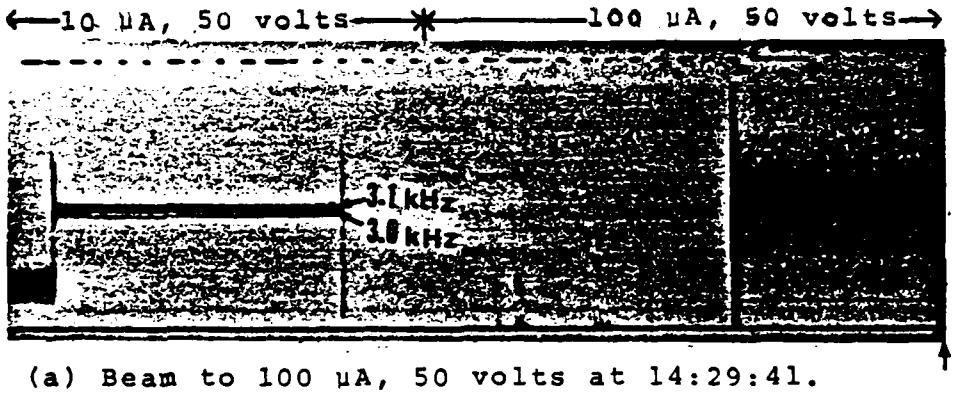

(a) Beam to 100 μA, 50 volts at 14:29:41.

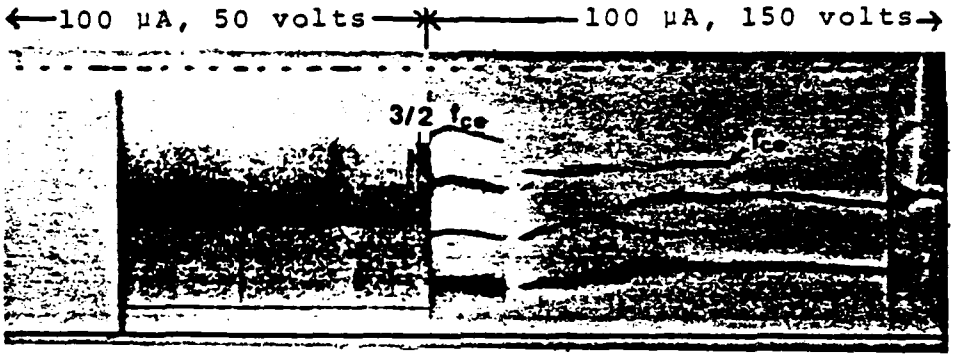

(b) Beam to 100 μA, 150 volts at 14:30:42.

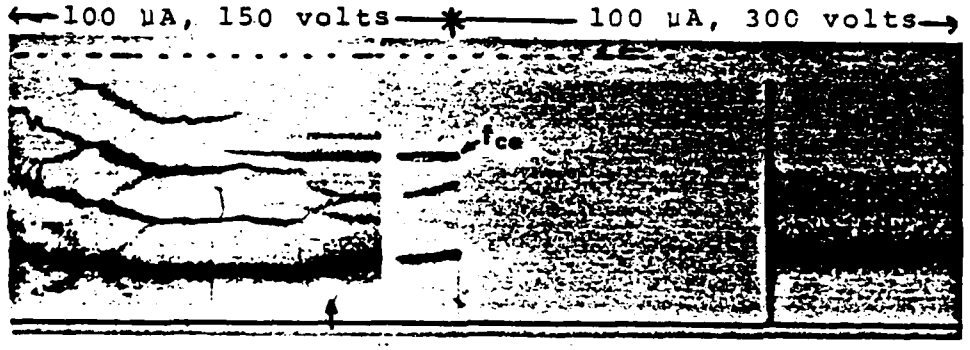

(c) Beam to 100 μA, 300 volts at 14:31:52.

Figure IIIB-9. Spectrogram for beam current of 100 μA; 50, 150, and 300 volts. (Arrows indicate times of line plots).

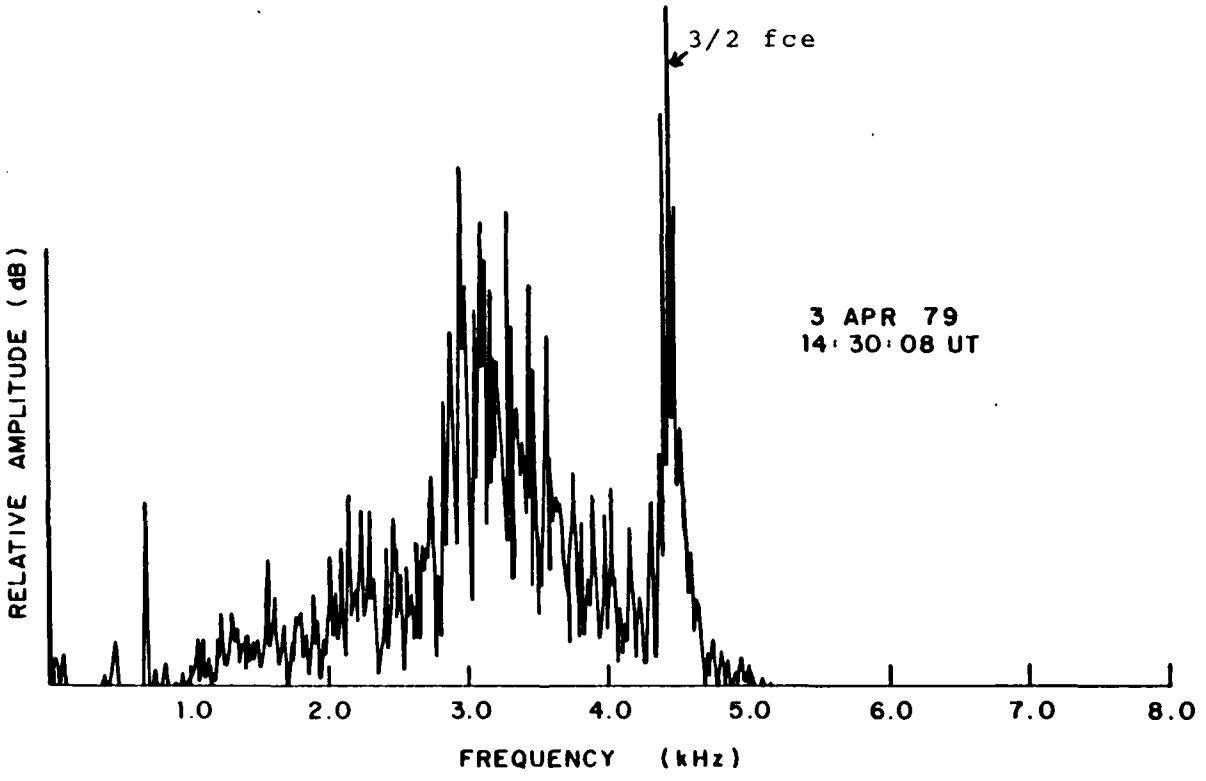

Figure IIIB-10. Magnetic receiver spectrum showing a sporadic signal (probably natural) at 4480 Hz. Beam is on at 100 μA, 50 volts.

IIIB-9b, shows the spectrum in line plot form. This signal is most likely a naturally occurring 3/2 fce, (fce=4200 Hz) and is seen again in Figure IIIB-9b just prior to the mode change. The broad spectrum at lower frequencies may also be naturally occurring. The beam energy is increased to 150 volts at 14:30:42 (Figure IIIB-9b). A signal at approximately 1350 Hz with harmonics at 2700, 4050 and 5400 Hz can be seen. This signal persists for the next few minutes in both the electric and magnetic field spectrograms (Figure IIIB-11). The 4-4.5 kHz signal attributed to electron gyrofrequency emissions can be seen superimposed on the more intense interference lines. A snapshot of the rapidly varying spectrum, Figure IIIB-12, shows the spectra measured at 14:31:45. The strongest amplitude frequencies are at 1380, 2730, 4110 and a weak signal at about 5480 Hz. These signals appear to be a fundamental frequency at 1380 Hz and its first three harmonics. The 4110 Hz signal is at or very near to the electron gyrofrequency.

We interpret the 100 μA, 150 V data as a result of a strong signal at 1300-1500 Hz, and harmonics generated within the receiver system. The AGC should nominally prevent this, but the response we observe here is

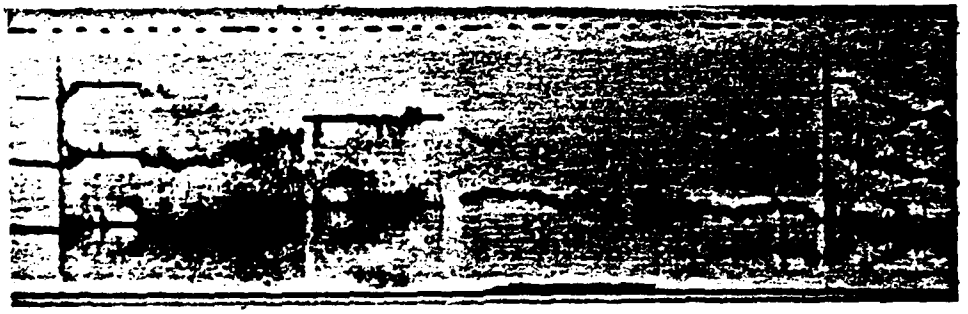

Figure IIIB-11. Plasma wave harmonic structure. Spectrogram taken at 14:31:12. Gun is on at 100 μA, 500 volts.

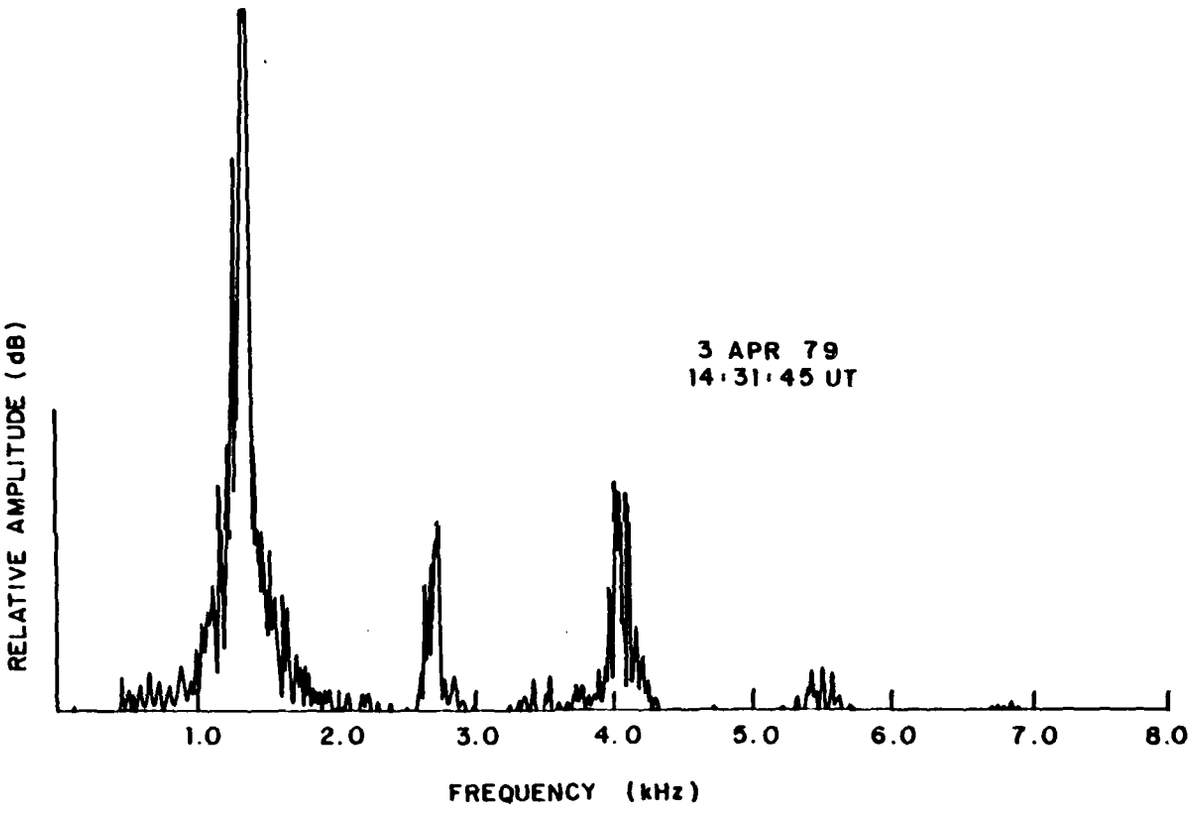

Figure IIIB-12. Magnetic receiver frequency spectrum of the harmonic structure seen in Figure IIIB-9c. Electron beam is on at 100 μA, 150 volts.

characteristic of an overdriven receiver. There appear to be "fce" lines, independent of the interference lines, distinguishable because they are not varying wildly in frequency. This latter variation may be associated with satellite spin, but the mode does not last long enough to determine this.

Returning to Figure IIIB-9c the beam energy is increased to 300 volts at 14:31:52 and the interference signal and its harmonics disappear from the electric receiver data. However, the magnetic data in Figure IIIB-9c shows a broad spectrum centered in the 1000-1500 Hz range the interference line occupied. The monochromatic signal and its harmonics reappeared for a few seconds (Figure IIIB-13) as a result of a change in the beam focus from low to medium. This was one of the few times the change in beam focus seemed to have any effect. Unlike the fce inferred for Day 200, this low fundamental frequency is well below the gyrofrequency, and does not have an obvious interpretation as a stimulated resonance of the plasma. Also, a monochromatic 4200 Hz line (i.e. fce) appears.

Figure IIIB-14 completes the gun parameter sequence. Shown are the spectrograms for the 100 μA; 500, 1500 and 300 volt settings of the electron gun beam parameters.

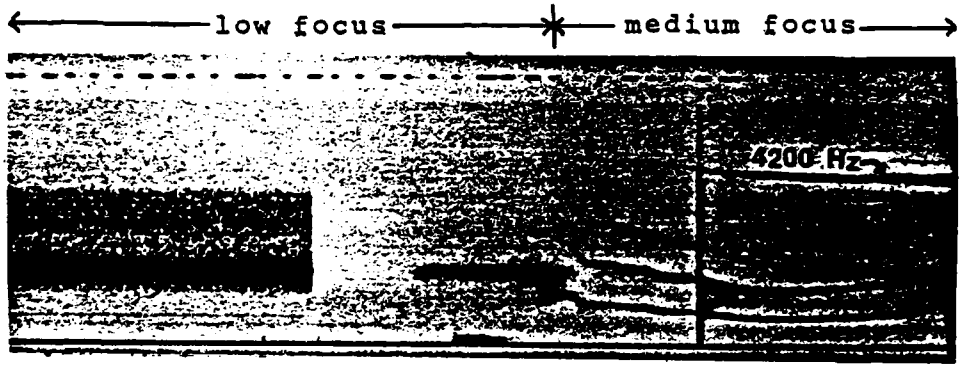

Figure IIIB-13. Spectrogram of focus change from low to medium at 14:32:30 for beam current of 100 μA and beam voltage of 300 volts.

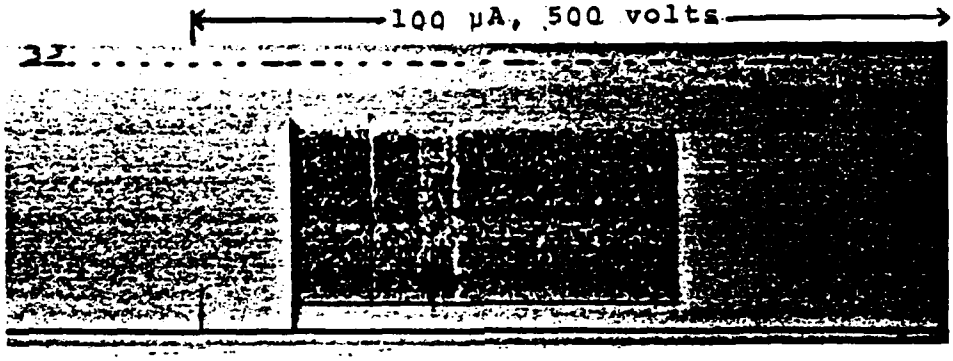

(a) Beam to 100 μA, 500 volts at 14:33:05.

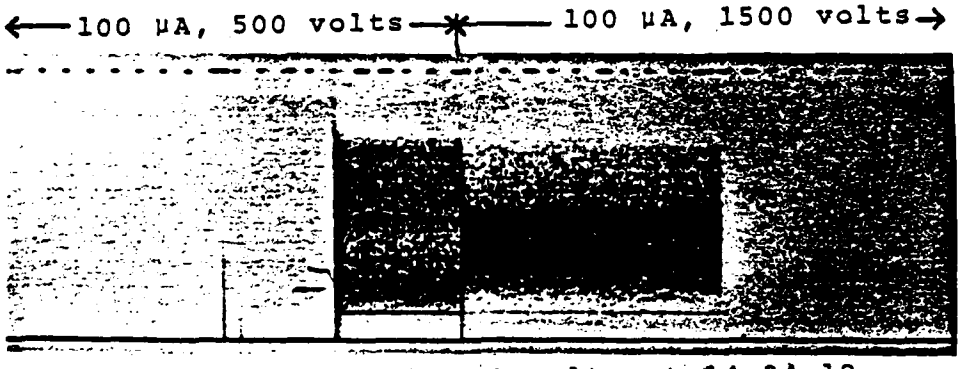

(b) Beam to 100 μA, 1500 volts at 14:34:18.

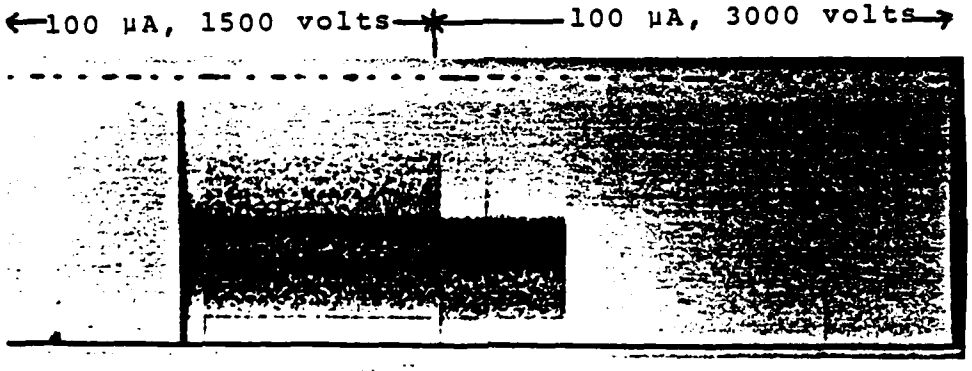

(c) Beam to 100 μA, 3000 volts at 14:35:28.

Figure IIIB-14. Spectrograms for beam current of 100 μA; 500, 1500 and 3000 volts.

At 14:33:05 the beam energy is increased to 500 volts (Figure IIIB-14a). This setting produces a diffuse background in the magnetic data and the tuning fork and 3 kHz interference lines are again distinguishable. Sporadic signals appear at 14:33:10 and at 14:33:50 at 1100 Hz which may be related to the harmonic signals seen earlier. The beam energy is increased to 1500 volts at 14:34:18 (Figure IIIB-14b). A diffuse background characterized the spectrogram between 700 to 5000 Hz with the maximum intensity signals centered at 2100 and 3000 Hz. At 14:35:28 (Figure IIIB-14c) the beam energy is increased to 3000 volts. The 3 kHz interference line appears to become the upper cutoff frequency for the broadband spectra in the magnetic data.

The beam is turned off at 14:36:30. The magnetic and electric spectra return to their pre-gun operation character. The tuning fork and 3 kHz interference lines are again the dominant feature in the spectrogram.

It has been shown that the gun operation affects the plasma wave data by noting the one to one correspondence the change to the gun parameters has on the changes in the plasma wave data. These effects vary but some common features have been identified. The interference lines at 700 Hz, 1400 Hz, 2100 Hz and 3 kHz are common features.

They do not appear to be tied to any particular setting of the gun, but do appear only in the magnetic receiver data. This would indicate that the intensity of these interference lines is very low and they are not sensed by the electric antenna. These interference lines come from other experiments on the satellite. Accordingly, they can usually be eliminated as features so that other more interesting, natural signals in the data can be studied.

The signals at 3130, 3715 and 3745 Hz that were observed at the 10 μA; 50, 150 and 300 volt modes appear to have been generated by the gun itself. They are only seen with the gun on and in the particular settings of the electron gun parameters. These signals may be linked to a voltage controlled oscillator (as suggested by Koons, 1987) that is part of the satellite experiment package. The change in frequency of the signal may be related to a change in the oscillator frequency as a result of the gun voltage change. Another characteristic of this signal was that it appeared in both the electric and magnetic field data. In other modes the common signals are seen only in the magnetic data.

The harmonic structure seen at the 100 μA current setting also appears to be gun related. It too appeared in both the magnetic and electric receiver data. The

signal appeared to be spin modulated, but the data are insufficient to be certain at this point.

During the sequencing of the gun parameters, the electron beam focus was also changed. Generally, the focus changes had little or no effect on the plasma wave data. Figure IIIB-13 showed one example where the focus change did induce an effect on the plasma wave data. The most significant change noted to the plasma wave data was enhancement of already present signals. Figure IIIB-15 shows an example of a change in focus from medium to high (1 μA, 50 volts). Note that only the intensities of the interference lines increases, no new or different signals are seen.

This section has provided samples of plasma wave data taken during various modes of operation of the electron gun. These examples can be used for future comparison to data taken during similar electron gun operations or experiments. These samples were taken in a particular satellite environment at a particular altitude so caution must be used when extrapolating comparisons of these examples to other data.

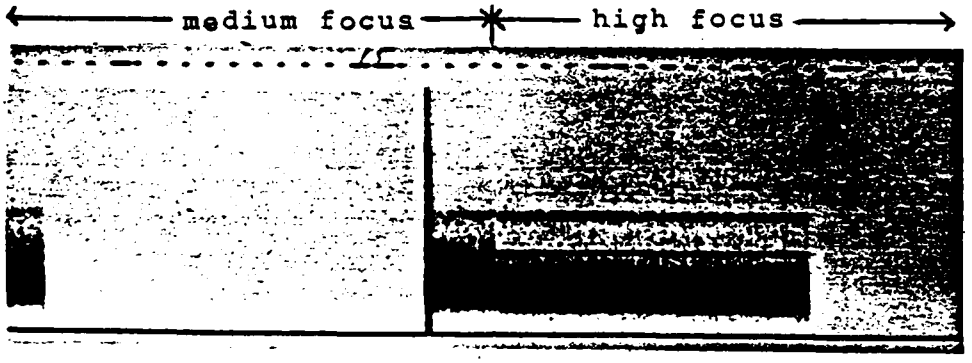

Figure IIIB-15. Spectrogram of focus change from medium to high at 14:15:05 for beam current of 1 μA and beam voltage of 50 volts.

C. OTHER OBSERVATIONS

The 10 μA mode of operation of the electron gun provided the most physically significant emissions that were observed. The 1 μA mode did not stimulate any obvious resonant emissions. The 100 μA mode generally overwhelmed the plasma wave data with receiver noise. On rare occasions (e.g. Figure IIIA-7) 100 μA data resembled gun off data. This section will discuss three additional periods when electron gun operations were conducted, with an emphasis on the plasma wave data taken at the 10 μA current setting.

On Day 111, 21 April 1979, between 0815 and 0838 UT the satellite was at L6.6, mean magnetic latitude of -1 degree and in eclipse. With the electron gun off the plasma wave data was typically characterized by the presence of the 3 kHz interference line and other structure (including driven harmonics). When the fun was turned on at 10 μA, 50 volts a new line near 3 kHz appeared. The new line was slightly lower in frequency than previously observed (approximately 2900 Hz). Beam parameter settings of 10 μA, 150 volts resulted in a corresponding monochromatic emission at 3.7 kHz. This behavior is similar to that seen on Day 93 (Figure IIIB-6). The emissions seen at 2.9 and 3.7 kHz are possibly

the same pair previously observed, as discussed in Chapter IIIB. The differences in frequency that are seen for the same gun parameters, i.e. 2900 Hz vice 3100 Hz for the 50 volts setting, may be due to temperature sensitive oscillators which cool in eclipse.

On Day 114, 24 April 1979, between 0735 and 0742 UT the electron gun was operated briefly at the 100 μA, 50 volts setting. The satellite was in eclipse, at L6.8 and magnetic latitude of 1 degree. The gun operations on this day for this mode have been discussed previously by Koons and Cohen (1982). The 3.0 kHz interference line was present in the magnetic receiver data with the gun on at 100 μA, 150 volts. In the electric receiver data a 3.1 kHz line is observed. Clear changes in frequency with antenna switching indicate the antennae, separated in space, are responding to different signals. The magnetic antenna is seeing the satellite generated line seen independent of the gun, while the electric antenna sees only the gun generated (or coupled) line. Later that same day electron gun operations were conducted with the satellite in sunlight. The 3.7 kHz line was again present at the 10 μA, 150 volt setting. One new line at 2400 Hz was seen when the gun was operated in the 10 μA, 50 volts mode.

These additional observations demonstrated the consistent presence of monochromatic emissions induced by the gun when operated in the lower voltage modes, particularly 50 and 150 volts. They appear to be related to an output frequency shift in a voltage controlled oscillator associated with the electron gun.

Table IV contains a summary of the distinct emissions seen in the plasma wave data examined to date. The emissions that could be identified as monochromatic and generally repeatable are tabulated by gun parameters.

IV. CONCLUSIONS

The operation of the electron gun had definite and predictable effects on the plasma wave data. The following was observed:

(a) On Day 200 the electron gun stimulated an emission at the electron gyrofrequency when operated at 10 μA, 50 volts. This signal resembled naturally occurring fce waves during the same period. Fluctuations in the frequency of the signal correlated with satellite spin and solar array current variations, and shows that the signal is a result of interactions between the electron beam and local plasma. This is consistent with inferences of ambient electron heating due to the beam (Olsen, 1986).

(b) The results of operation of the gun at 100 μA, 50 volts were similar to those with the gun off, on Day 200. This means there is a density/energy effect on wave growth.

(c) On other days, the gun operation apparently couples electron gun generated interference to the plasma wave instruments, independently of

local plasma characteristics. The characteristics of the plasma wave data were presented for the operation of the electron gun at different parameters. Common features can be identified for comparison to future data:

(1) The interference lines generated by the tuning fork oscillator at 700, 1400 and 2100 Hz are routinely seen in the magnetic receiver data.

(2) Operation of the electron gun tends to mask the reception of the tuning fork interference lines.

(3) A satellite generated interference line at 3 kHz is commonly seen, independent of the setting of the electron gun.

(4) Operation of the electron gun at 10 μA; 50, 150 and 300 volts generates a signal that most probably has a source in a voltage controlled oscillator in the electron gun. It is possible that coupling to other circuits in the satellite is enhanced by the beam.

(5) Higher voltage settings at 10 μA resulted in significantly different features. Broad

diffuse spectra were seen instead of monochromatic spectra.

(6) Changes in the electron beam focus generally acted only to enhance emissions that were already present. No new interference lines were generated.

The samples of the plasma wave data taken during the various modes of operation of the electron gun can be used to compare with data from similar experiments. As more data are collected and compiled, better understanding of beam-plasma interactions can be realized.

Implications of this work for use of electron beams for satellite charge control are:

(a) electron beam changes the electron density

(b) stimulated waves generate electron transport so that changes to the net current to and from the satellite is not what would be expected simply by adding the electron beam effects. The electron beam may not, in fact, escape from the satellite.

APPENDIX

TABLE I. P78-2 (SCATHA) EXPERIMENT

IDENTIFICATION	TITLE
SC1	Engineering Experiment Plus VLF and HF Receivers
SC2	Spacecraft Sheath Fields Plus Energetic Ions
SC3	High Energy Particle Spectrometer
SC4	Satellite Electron And Positive Ion Beam System
SC5	Rapid Scan Particle Detector
SC6	Thermal Plasma Analyzer
SC7	Light Ion Mass Spectrometer
SC8	Energetic Ion Composition Experiment
SC9	UCSD Charged Particle Experiment
SC10	Electric Field Detector
SC11	Magnetic Field Monitor
ML12	Spacecraft Contamination Plus Thermal Control Materials Monitoring
TPM	Transient Pulse Monitor

TABLE II

Day 201 20 JUL 79

TIME	SC4-1 COMMAND
22:53:40	Initialize and Off
22:54:54	System On
22:55:00	Beam On
22:55:37	Beam Current to 10 μA
23:02:28	Beam Current to 100 μA
23:03:15	Beam Current to 10 μA
23:07:41	Beam Off
23:18:31	Beam On 10 μA
23:21:34	Beam Current to 100 μA
23:21:58	Beam Current to 10 μA
23:23:48	Beam Off
23:26:03	System Init. and Off

TABLE III

DAY 93 3 APR 79

TIME	SC4-1 COMMAND
14:13:24	0.01 MA Beam Current
14:13:34	Power On
14:14:04	Beam On
14:14:34	1 μA, 50 V, M
14:15:05	Focus to High
14:15:34	Focus to Low
14:15:43	Increase Voltage to 150 V
14:17:00	Focus to High
14:17:09	Increase Voltage to 300 V
14:17:39	Focus to Med
14:18:09	Focus to Low
14:18:19	Increase Voltage to 500 V
14:19:03	Focus to Med
14:19:33	Focus to High
14:19:44	Increase Voltage to 1500 V
14:20:26	Focus to Med
14:21:03	Increase Beam Energy to 3000 V
14:21:31	Focus to High
14:22:10	Focus to Med
14:22:19	Beam Energy to 50 V
14:22:27	Beam Current to 10 μA
14:23:20	Focus to High
14:23:36	Beam Voltage to 150 V
14:24:38	Focus to Low
14:24:47	Beam Voltage to 300 V
14:25:17	Focus to Med
14:25:47	Focus to High
14:25:58	Beam Voltage to 500 V
14:26:27	Focus to Med
14:26:57	Focus to Low
14:27:07	Beam Voltage to 1500 V
14:27:47	Focus to Med
14:28:20	Focus to High
14:28:29	Beam Energy to 3000 V
14:28:57	Focus to Med
14:29:29	Beam Voltage to 50 V
14:29:41	Beam Current to 100 μA
14:30:12	Focus to High
14:30:42	Beam Voltage to 150 V
14:31:12	Focus to Med
14:31:42	Focus to Low
14:31:52	Beam Voltage to 300 V

14:32:30	Focus to Med
14:32:56	Focus to High
14:33:05	Beam Energy to 500 V
14:33:38	Focus to Med
14:34:08	Focus to Low
14:34:18	Beam Energy to 1500 V
14:34:48	Focus to Med
14:35:18	Focus to High
14:35:28	Beam Energy to 3000 V
14:35:58	Focus to Med
14:36:36	Off

TABLE IV

Gun Setting		Frequencies (Hz)
off		700, 1400, 2100, 3000
1 μA,	50 volts	700, 2100, 3000
	150 volts	----------
	300 volts	----------
	500 volts	700, 2100, 3000
	1500 volts	700, 2100, 3000
	3000 volts	----------
10 μA,	50 volts	2400, 2745, 2900, 3000, 3130
	150 volts	3700, 3745
	300 volts	3000, 3715
	500 volts	700, 1400, 2100, 3000, 4000, 5800
	1500 volts	----------
	3000 volts	----------
100 μA,	50 volts	700, 2100, 3000
	150 volts	1350, 3100,4200
	300 volts	4200
	500 volts	700, 1400, 2100, 3000
	1500 volts	----------
	3000 volts	----------

LIST OF REFERENCES

Akai, K., Electron Beam--Plasma Interaction Experiment in Space, ISAS Research Note 285, The Institute of Space and Astronautical Science, Komaba, Meguro-ku, Tokyo, Japan, undated.

Bernstein, W., H. Leinbach, Herbert Cohen, P.S. Wilson, T.N. Davis, T. Hallinan, B. Baker, J. Martz, R. Zeimke, and W. Huber, Laboratory Observations of RF Emissions at wpe and (n+½)wce in Electron Beam-Plasma and Beam-Beam Interactions, Journal of Geophysical Research, V. 80, pp. 4375-4379, 1975.

Chen, Francis F., Introduction to Plasma Physics and Controlled Fusion, Vol. 1, 2nd ed., Plenum Press, New York and London, 1985.

DeForest, Sherman E., Spacecraft Charging at Synchronous Orbit, Journal of Geophysical Research, V. 77, pp. 651-659, 1972.

Fennell, J.F., "Description of the P78-2 (SCATHA) Satellite and Experiments", in The IMS Source Book: Guide to the International Magnetospheric Study Data Analysis, edited by C.T. Russell and D.J. Southwood, p. 65, AGU, Washington, D.C., 1982.

Garrett, H.B., "The Charging of Spacecraft Surfaces", in Reviews of Geophysics and Space Physics, V. 19, pp. 577-616, November 1981.

Grard, R., K. Knott, and Pedersen, Spacecraft Charging Effects, Space Science Reviews, V. 34, pp. 289-304, 1983.

Gussenhoven, M.S., E.G. Mullen and D.A. Hardy, Artificial Charging of Spacecraft Due to Electron Beam Emission, presented at IEEE mtg, August 1987.

Kawashima, N., S. Sasaki, O. Kaneko, Y. Nakamura, H. Kubo, T. Obayashi and S. Miyatake, Experiments of Electron Beam from Rocket, Institute of Space and Aeronautical Science, Tokyo, Japan, 1976.

Kawashima, N., and the JIKIKEN (Exos-B) CBE Project Team, Wave Excitation in Electron Beam Experiment on Japanese Satellite "JIKIKEN (Exos-B)", The Institute of Space and Aeronautical Science, Komaba, Meguro-ku, Tokyo, Japan, undated.

Kawashima, N., S. Sasaki, K.I. Oyama, W.J. Raitt, P.R. Williamson and P.M. Banks, Further Analysis of the Results from a Series of Tethered Rocket Experiments, paper presented at the International Conference on Tethers, October, 1987.

Koons, H.C. and H.A. Cohen, Plasma Waves and Electrical Discharges Stimulated by Beam Operations on a High Altitude Satellite, in Artificial Particle Beams in Space Plasma Studies, edited by Bjorn Grandal, Plenum Press, New York, pp. 111-120, 1982.

Koons, H.C. and B.C. Edgar, Observations of VLF Emissions at the Electron Gyrofrequency, Journal of Geophysical Research, V. 90, pp. 10961-10967, 1985.

Koons, H.C., B.C. Edgar, J.F. Fennell and D.J. Gorney, Observations of Electron Cyclotron Harmonics Emissions Associated with Field-Aligned Electron Beams, Journal of Geophysical Research, V. 92, pp. 7531-7537, 1987.

Koons, H.C., Private communication, November 1987.

Lebreton, J.P., R.Torbert, R. Anderson and C. Harvey, Stimulation of Plasma Waves by Electron Guns on the ISEE-1 Satellite, in Artificial Particle Beams in Space Plasma Studies, edited by Bjorn Grandal, Plenum Press, New York, pp. 133-146, 1982.

Ledley, B., Private communication, November 1987.

Margot-Chaker, J. and A.G. McNamara, "A Study of the Ionospheric Disturbance Induced by an Injected Electron Beam", Journal of Geophysical Research, V. 91, pp. 7079-7088, 1986.

Matsumoto, Hiroshi, S. Miyatake, and I. Kimura, "Rocket Experiment on Spontaneously and Artificially Stimulated VLF Plasma Waves in the Ionosphere", Journal of Geophysical Research, V. 80, pp. 2829-2834, 1975.

Olsen, R.C., "Modification of Spacecraft Potentials by Thermal Electron Emission on ATS-5", Journal of Spacecraft and Rockets, V. 18, pp. 527-532, 1981.

Olsen, R.C., "Experiments in Charge Control at Geosynchronous Orbit--ATS 5 and ATS 6", Journal of Spacecraft and Rockets, V. 22, pp. 254-264, 1985.

Olsen, R.C., Electron Beam Experiments at High Altitudes, presented at the NATO/AGARD Conference on the Aerospace Environment at High Altitudes and its Implications for Spacecraft Charging and Communications, The Hague, The Netherlands, 2-6 June 1986, Agard-CP-406, pp. 10-1 to 10-8, 1986.

Olsen, R.C., D.R. Lowery and L.E. Weddle, "Plasma Wave Observations During Electron and Ion Gun Experiments", submitted to AIAA for publication in Journal of Spacecraft and Rockets, 1987.

INITIAL DISTRIBUTION LIST

		No. Copies
1.	Defense Technical Information Center Cameron Station Alexandria, Virginia 22304-6145	2
2.	Library, Code 0142 Naval Postgraduate School Monterey, California 93943-5002	2
3.	Department Chairman, Code 61 Department of Physics Naval Postgraduate School Monterey, California 93943	2
4.	Dr. R. C. Olsen, Code 61OS Department of Physics Naval Postgraduate School Monterey, California 93943	20
5.	Dr. S. Gnanalingam, Code 61GM Department of Physics Naval Postgraduate School Monterey, California 93943	1
6.	Ms. D. E. Donatelli Space Physics Division Air Force Geophysics Laboratory/PH Hanscom AFB, Massachusetts 01731	1
7.	Dr. R. Sagalyn Space Physics Division Air Force Geophysics Laboratory/PH Hanscom AFB, Massachusetts 01731	1
8.	Mr. G. Mullen Space Physics Division Air Force Geophysics Laboratory/PHP Hanscom AFB, Massachusetts 01731	1
9.	Dr. S. Lai Space Physics Division Air Force Geophysics Laboratory/PH Hanscom AFB, Massachusetts 01731	1

10. Dr. B. Burke 1
Space Physics Division
Air Force Geophysics Laboratory/PHA
Hanscom AFB, Massachusetts 01731

11. Dr. N. Maynard 1
Space Physics Division
Air Force Geophysics Laboratory/PH
Hanscom AFB, Massachusetts 01731

12. Mr. H. A. Cohen 1
W. J. Schafer Associates
1901 North Fort Meyer Drive
Arlington, Virginia 22209

13. Mr. R. Gracen Joiner 1
Office of Naval Research, Code 1114
800 North Quincy Street
Arlinton, Virginia 22217-5000

14. Dr. H. C. Koons 3
Space Sciences Laboratory
The Aerospace Corporation, M2/260
P. O. Box 92957
Los Angeles, California 90009

15. Dr. J. Roeder 2
Space Sciences Laboratory
The Aerospace Corporation, M2/260
P. O. Box 92957
Los Angeles, California 90009

16. Dr. E. C. Whipple 1
Center for Astrophysics and Space Science
University of California at San Diego
La Jolla, California 92093

17. Dr. C. E. McIlwain 1
Center for Astrophysics and Space Science
University of California at San Diego
La Jolla, California 92093

18. Dr. J. Hyman 1
Hughes Research Lab
3011 Malibu Canyon Road
Malibu, California 90265

19. Dr. T. Williamson — 1
Hughes Research Lab
3011 Malibu Canyon Road
Malibu, California 90265

20. Dr. S. Shawhan — 1
NASA Headquarters/E
Washington, DC 20546

21. Dr. C. K. Purvis — 1
MC 302-1
NASA Lewis Research Center
21000 Brookpark Road
Cleveland, Ohio 44135

22. Dr. J. Kolecki — 1
MC 302-1
NASA Lewis Research Center
21000 Brookpark Road
Cleveland, Ohio 44135

23. Dr. C. R. Chappell — 1
NASA Marshall Space Flight Center
Huntsville, Alabama 35812

24. Dr. T. E. Moore, ES53 — 1
NASA Marshall Space Flight Center
Huntsville, Alabama 35812

25. Dr. J. H. Waite, ES53
NASA Marshall Space Flight Center
Huntsville, Alabama 35812

26. Dr. D. Hastings — 1
Department of Aeronautics and Astronautics
Massachusetts Institute of Technology
Cambridge, Massachusetts 02139

27. Dr. I. Katz — 2
S - Cubed
P. O. Box 1620
La Jolla, California 92038-1620

28. Dr. J. Raitt — 1
CASS
Utah State University
Logan, Utah 84322

29. Professor Nobuki Kawashima 1
Institute of Space and Astronautical Science
Komaba 4 - chome
Meguro - ku
Tokyo, Japan 153

30. Professor W. Riedler 1
Institute fuer Weltraumforschung Oesterreichische Akademieder Wissenschaften
Inffeldgasse 12
A - 8810 Graz, Austria

31. Dr. K. Torkar 1
Institute fuer Weltraumforschung Oesterreichische Akademieder Wissenschaften
Inffeldgasse 12
A - 8810 Graz, Austria

32. Dr. R. Schmidt 1
Space Science Department
ESA/ESTEC
Noordwijk, The Netherlands

33. Dr. A. Pedersen 2
Space Science Department
ESA/ESTEC
Noordwijk, The Netherlands

34. Lcdr D.R. Lowery, USN 1
P.O. Box 5212
Marshville, N.C. 28103

35. Dr. W. F. Denig 1
Space Physics Division
Air Force Geophysics Laboratory/PHG
Hanscom AFB, Massachusetts 01731

36. Dr. N. Omidi 1
IGPP
University of California at Los Angeles
Los Angeles, California 90024

37. Dr. Maha Ashour - Abdalla 1
IGPP
University of California at Los Angeles
Los Angeles, California 90024

38. Dr. R. R. Anderson 1
Department of Physics and Astronomy
University of Iowa
Iowa City, Iowa 52242

END